

NASA-TM-X

72820 Experimental measurements of the ground cloud effluents and cloud growth during the February 11, 1974, Titan-Centaur launch at Kennedy Space Center

## NASA TECHNICAL MEMORANDUM

NASA TM X-72820

NASA TM X-72820

EXPERIMENTAL MEASUREMENTS OF THE GROUND CLOUD EFFLUENTS AND CLOUD GROWTH  
DURING THE FEBRUARY 11, 1974, TITAN-CENTAUR LAUNCH AT  
KENNEDY SPACE CENTER

Roger B. Stewart\*, Ronald J. Sentell,

and

Gerald L. Gregory

FL2827

February 1976

30SPW/XPOT TECHNICAL LIBRARY  
BLDG. 7015  
806 13th ST., SUITE A  
VANDENBERG AFB, CA 93437-5223



\* Deceased

This Informal documentation medium is used to provide accelerated or special release of technical information to selected users. The contents may not meet NASA formal editing and publication standards, may be revised, or may be incorporated in another publication.

NATIONAL AERONAUTICS AND SPACE ADMINISTRATION  
LANGLEY RESEARCH CENTER, HAMPTON, VIRGINIA 23665

(NASA-TM-X-72820) EXPERIMENTAL MEASUREMENTS  
OF THE GROUND CLOUD GROWTH DURING THE 11  
FEBRUARY 1974, TITAN-CENTAUR LAUNCH AT  
KENNEDY SPACE CENTER (NASA) 50 p 14.00

N76-22720

Unclas  
CSCI 13E G3/45 26879

1. Report No. TM X 72820		2. Government Accession No.		3. Recipient's Catalog No.	
4. Title and Subtitle Experimental Measurements of the Ground Cloud Effluents and Cloud Growth During the February 11, 1974 Titan-Centaur Launch at Kennedy Space Center				5. Report Date February 1976	
				6. Performing Organization Code	
7. Author(s) * Roger B. Stewart, Ronald J. Sentell and Gerald L. Gregory				8. Performing Organization Report No.	
9. Performing Organization Name and Address NASA Langley Research Center Hampton, VA 23665				10. Work Unit No. 989-15-20-01	
				11. Contract or Grant No.	
12. Sponsoring Agency Name and Address National Aeronautics and Space Administration Washington, DC 20546				13. Type of Report and Period Covered Technical Memorandum	
				14. Sponsoring Agency Code	
15. Supplementary Notes * Deceased					
16. Abstract  This report summarizes the effluent measurements and ground cloud behavior during the NASA launch vehicle effluent monitoring experiments at the Titan-Centaur proof flight test. The Titan-Centaur was launched from Kennedy Space Center on February 11, 1974 at 0948 eastern daylight time. The objectives of the experiment were to gather ground level effluent measurements for comparison with NASA models for predicting effluent ground level concentrations and cloud behavior. Results obtained provide a basis for an evaluation of such key model inputs as cloud rise rate, stabilization altitude, crosswind growth, volume expansion, and trajectory. Ground level effluent measurements were limited due to changing meteorological conditions, incorrect instrument location, and operational problems. Based on the measurement results, operational changes are defined.					
17. Key Words (Suggested by Author(s)) (STAR category underlined) Effluent sampling                      STAR 45 Rocket vehicle exhaust Titan III exhaust effluents				18. Distribution Statement Unclassified - unlimited	
19. Security Classif. (of this report) Unclassified		20. Security Classif. (of this page) Unclassified		21. No. of Pages 49	22. Price* \$3.75



EXPERIMENTAL MEASUREMENTS OF THE GROUND CLOUD EFFLUENTS  
AND CLOUD GROWTH DURING THE FEBRUARY 11, 1974, TITAN-CENTAUR  
LAUNCH AT KENNEDY SPACE CENTER

By Roger B. Stewart, Ronald J. Sentell and Gerald L. Gregory  
Langley Research Center

SUMMARY

This report summarizes the effluent measurements and ground cloud behavior during the joint NASA Langley Research Center (LaRC), Marshall Space Flight Center (MSFC), and Kennedy Space Center (KSC) booster effluent monitoring experiments during the February 11, 1974 Titan-Centaur proof flight test. The Titan-Centaur was launched from Kennedy Space Center (Launch Complex 41) on February 11, 1974 at 1348 UT (0948 EDT).

This experiment included the in situ ground level measurements of the exhaust effluents from the Titan III-E solid rocket boosters. Simultaneous visible spectrum photographic pictures of the ground cloud rise and direction of travel, as well as infrared imaging of the cloud were obtained to study the cloud rise, growth, and thermal history within the surface mixing layer. The MSFC multilayer diffusion model predictions of cloud growth, direction of travel, and expected ground level effluent concentrations were made prior to launch and post launch using measured meteorological conditions.

The objectives of the experiment were to gather ground level effluent measurements for a comparison with the MSFC diffusion model predictions as well as to obtain cloud rise and growth data to aid in reducing the uncertainty associated with several empirical inputs to the diffusion model. Additional objectives were to define and refine operational strategy and instrumentation planned for future monitoring experiments at KSC.

Results obtained provide a basis for an evaluation of such key model inputs as cloud rise rate, stabilization altitude, crosswind growth, volume expansion, and trajectory. Ground level effluent measurements were limited due to changing meteorological conditions, incorrect instrument location, and operational problems. Operational changes were defined to be in the areas of increasing the number of sampling sites at sea, re-positioning of sampling seacraft after launch, and specification of seacraft operational characteristics.

INTRODUCTION

The National Aeronautics and Space Administration is actively pursuing tropospheric and stratospheric environmental studies in conjunction with rocket firings. The tropospheric program is aimed at measuring and predicting

REPRODUCIBILITY OF THE  
ORIGINAL PAGE IS POOR

the impact of ground clouds produced at launch on the ground level air quality. The Launch Vehicle Effluents (LVE) monitoring program is conducted by the NASA Langley Research Center with intercenter support from Marshall Space Flight Center (MSFC) and Kennedy Space Center (KSC). The goal of the LVE program is to assess the applicability and accuracy of diffusion models for predicting the dispersion of exhaust effluents from NASA's current and future launch vehicles. The objectives of the program are to develop data to be used in the establishment of potential launch constraints and to develop in-house expertise in the areas relating to the environmental impact of launch activities. The approach employed to meet these objectives is that of measuring rocket exhaust products produced by large solid rocket motor launch vehicles at ground level and within the "stabilized ground cloud" formed in the troposphere as the result of the launch. The measurements will be used to make direct comparisons with the diffusion models and NASA Rocket Plume Codes that are used to predict effluent composition and concentrations. In addition, many of the empirical inputs required by the models can be measured in association with the ground level effluent measurements.

This report summarizes the effluent measurements and ground cloud behavior during the February 11, 1974 Titan-Centaur proof flight test. The Titan-Centaur was launched from Kennedy Space Center (Launch Complex 41) on February 11, 1974, at 1348 UT (0948 EDT).

This experiment included the in situ ground level measurements of the exhaust effluents from the Titan III-E solid rocket motor boosters. Simultaneous visible spectrum photographic pictures of the ground cloud rise and direction of travel, as well as infrared imaging of the cloud were obtained to study the cloud rise, growth, and thermal history within the surface mixing layer. The MSFC multilayer diffusion model predictions of cloud growth, direction of travel, and expected ground level effluent concentrations were made prior to launch and post launch using measured meteorological conditions.

The Authors acknowledge the cooperation and support of Kennedy Space Center personnel and U.S. Air Force personnel during the experimental measurement program.

#### OBJECTIVES

The objectives of the experiment were to gather ground level effluent measurements for a comparison with the MSFC diffusion model predictions as well as to obtain cloud rise and growth data to aid in reducing the uncertainty associated with several empirical input values for the diffusion model. Additional objectives were to define and refine operational strategy and instrumentation planned for future monitoring experiments at KSC.

## SYMBOLS

AFETR - Air Force Eastern Test Range

$D_c$  - Corrected particle dosage,  $\mu\text{gm-sec}/\text{m}^3$

EDT - Eastern Daylight Time

F - Sample flow rate,  $\text{m}^3/\text{min}$  or  $\text{m}^3/\text{sec}$

FM - Frequency modulated

KSC - Kennedy Space Center

LaRC - Langley Research Center

LC-41 - Launch Complex 41

LVE - Launch Vehicle Effluent

MSFC - Marshall Space Flight Center

NAA - Neutron Activation Analysis

NASA - National Aeronautics and Space Administration

ppm - parts-per-million by volume

SRM - solid rocket motor

T - Time prior to launch

TVC - Thrust vector control

t - sample time, min.

UCS - universal camera site

UT - universal Time

W - Corrected weight gain,  $\mu\text{gm}$

$W_H$  - Handling effects correction factor,  $\mu\text{gm}$

$W_S$  - uncorrected sample weight gain,  $\mu\text{gm}$

$x_A$  - normal ambient particle concentration,  $\mu\text{gm}/\text{m}^3$

## PROGRAM DESCRIPTION

### Launch Vehicle

Figure 1 shows the Titan-Centaur just after lift-off. The rocket exhaust from about the first 20 seconds of burn is contained in the ground cloud that forms and rises to a stabilization height within 5 minutes after ignition. The Titan III-E uses two solid rocket motor (SRM) boosters that together have a mass flow rate at lift-off of  $4.16 \times 10^6$  grams per second ( $9.173 \times 10^3$  pounds per second). In addition, the thrust vector control (TVC) system expends nominally  $4.5 \times 10^4$  grams per second (100 pounds per second of nitrogen tetroxide ( $N_2O_4$ ) into the nozzle flows of both boosters during the formation of the ground cloud. The TVC mass flow rate and booster mass flow rates are nearly constant during this time period. The SRM propellant consists of an ammonium perchlorate oxidizer, an aluminized synthetic-rubber binder fuel, and various other additives to stabilize mass and to control the burning rate. The major constituents after combustion are hydrogen chloride (HCl), aluminum oxide ( $Al_2O_3$ ), carbon monoxide (CO), carbon dioxide ( $CO_2$ ), molecular nitrogen ( $N_2$ ), molecular hydrogen ( $H_2$ ), and water ( $H_2O$ ) vapor. The thrust vector control constituents decompose in the rocket exhaust to nitric oxide (NO) and oxygen ( $O_2$ ). The motor exit plane composition (Ref. 1) is shown in table 1, along with the products formed after afterburning and air entrainment in the first kilometer of the plume (Ref. 2). As shown in the table, at 1 kilometer downstream from the nozzle exit plane the exhaust effluents have been greatly diluted by air entrainment and the majority of CO has been afterburned to  $CO_2$ .

### Prelaunch Effluent Predictions

Prelaunch effluent predictions using the dispersion model (Ref. 3) and meteorological forecasts, starting at T-3 days and continuing to T-2 hours, were used to design the effluent sampling experiment. Meteorological forecasts were based on local wind tower observations, local rawinsonde releases, and synoptic weather data as supplied by the National Weather Service network. Marshall Space Flight Center (MSFC) personnel provided both the effluent predictions and the meteorological forecasts. Table II briefly summarizes the prelaunch predictions from T-3 days to T-2 hours. Each prediction was furnished in a standard format and, as discussed in the next section, was used to design various phases of the effluent sampling experiments.

### Locations of Instruments

The azimuth and distance from the launch pad of each of the 24 sampling sites used in this effluent sampling study are shown in figure 2 and table III. All sites except site MM were selected on the basis of prelaunch dispersion predictions and meteorological forecasts. Site MM, a permanent site for all LC-41 launches, is located on the launch-complex perimeter road.

Because of the location of LC-41 and the frequency of westerly winds, there is always a high probability that the ground cloud will drift towards the ocean. In order to cover this possibility, four seacraft were obtained as sampling platforms. As shown in figure 3, the T-1 day prediction showed the effluent cloud moving towards the ocean. Based on this prediction, procedures were implemented to prepare the seacraft for a sampling mission. The final commitment to the seacraft sampling was withheld until after T-8 hour prediction. Between T-8 hours and T-6 hours, equipment was loaded aboard the four seacraft (instrument set P-1 through P-4) with seacraft departure occurring approximately T-6 hours. As shown in figure 3, the predicted cloud path from T-2 days to T-6 hours showed a continual shift to the north until at T-6 hours the predicted cloud path was north of the launch vehicle flight path. Thus at T-5 1/2 hours the boats were directed north of the vehicle flight path ( $104^\circ$ ) with planned sampling positions as shown in figure 4. Three of the four sampling positions were within the seacraft prohibited zone (see Fig. 4), which is an area centered about the vehicle flight path where no seacraft can be located at vehicle lift-off due to safety considerations. Thus, these three seacraft were assigned holding positions outside of this zone and at T+90 seconds were released to proceed to the desired sampling position within the seacraft prohibited zone. However, by T-2 hours, the forecasted (Table II) cloud path was again south of the vehicle flight path at a predicted azimuth of  $110^\circ$ . By this time, all seacraft were in their sampling positions or holding positions north of the prohibited zone, and range safety requirements prevented moving the seacraft to the south side of the prohibited zone. Thus at T-1 1/2 hours, new sampling positions were radioed to the seacraft showing the final sampling locations south of the vehicle flight path and considerable distance from the seacraft holding positions. Figure 5 shows the planned sampling positions as well as the actual seacraft path. As shown in figure 5, seacraft P-2 was not vectored south at T+90 seconds. This decision was based on the sea state, (rough) sea worthiness (poor) of the seacraft, and personnel safety. Seacraft P-3 was capable of only 2-3 knots in the rough sea condition, and thus could only be vectored a short distance south. In addition, seacraft P-4, was given instructions to deviate from the planned sampling mission (Fig. 5) and to attempt to intersect the cloud using visual observations from the seacraft. This decision was made after it was determined that P-4 could not arrive at its planned sampling station prior to cloud arrival at the location. P-4 arrived at the predicted cloud trajectory at about T+40 minutes and observed the cloud to be several kilometers to the south and beyond their location. As will be shown later in this report, the launch cloud went further south than the  $110^\circ$  azimuth, and seacraft P-1 through P-4 did not intercept the launch effluent cloud. It should be noted here, that the meteorological forecasts used in this siting plan were adequate, and that the shift in predicted cloud path back to the south was only identifiable at T-2 hours. Meteorological forecasts (from two different sources) prior to T-2 hours indicated continual shift of the cloud path to the north of the vehicle flight path.

The other 19 sampling sites were selected using the model predictions and meteorological forecasts from T-8 hours to T-1 hours. These site selections are summarized below:

FL2827  
30SPW/XPOT TECHNICAL LIBRARY  
BLDG. 7015  
806 13th ST SUITE A  
VANDENBERG AFB, CA 93437-5223

T-8 Hour Prediction. This prediction was used to select instrument sites S-1 through S-15. The sampling philosophy was to locate these sites along the only existing road between LC-41 and the ocean. The sites were located at 0.1 mile increments resulting in azimuths from the pad ranging from 3° to 134°. These site selections were biased to the north based on the expected continual shift of the predicted cloud path to the north. The purpose of sites S-1 through S-15 in this sampling plan was to locate the effluent cloud centerline as it crossed the coast.

T-6 Hour Prediction. This prediction was used to select sites CC, DD, FF, and P-5. Unlike sites S-1 through S-15, which were battery powered, sites CC, DD, FF, and P-5 required hardline electrical power. In addition, instrument sets CC, DD, and FF required hardline control circuits for instrument activation and deactivation. Sites CC, DD, and FF were selected as they were the sites closest to the 92° (T-6 hour) predicted cloud path with the required electrical and control hardlines. Site P-5 was selected as a background site, as there were no available (capable of being manned at lift-off) sites between LC-41 and the ocean near the predicted cloud path.

T-2 Hour Prediction. This prediction was used to update the sampling schedule for all instrument sites and provided cloud path and altitude data for the optical tracking teams.

As previously discussed, the post launch effluent predictions using the MSFC dispersion model and the actual launch time meteorological data are presented in the Results Section of this report.

#### Measurement Systems

Effluent Measurement Systems. The instruments used at each sampling site are shown in table IV. The sampling capabilities of each type of instrument and any laboratory analysis required in reporting the data are described in table V. References describing the operation of the various instruments are given in column 1 of table V. All instruments are commercially available and their characteristics well documented. Where possible the performance parameters given in table V are based on laboratory and field experience with each sampling unit. In lieu of this experience, manufacturer values are quoted. Particle analysis was directed at: (1) the identification of chemical elements and their relative abundance using neutron activation analyses; the determination of mass loading using gravimetric analysis; and (3) the determination of particle size using microscopic counting techniques. Appropriate background samples were taken prior to launch using selected instruments and are presented in the Results Section.

Optical System. Three metric tracking units (Askania cameras) were employed to determine the rise and direction of travel of the effluent ground cloud as a function of time. In addition, a time sequenced camera (Massalblad) was positioned at each of the metric tracking sites to obtain color still photographs of the cloud at 10 second intervals after launch. The location of the tracking units and cameras are shown in figure 6.

An infrared imaging system was mounted on top of the metric tracking unit at Universal Camera Site 9 (see Fig. f). The imager scans with a field frequency of 16 per second in the wave length region from 2 to 5.6 microns. The device has a line frequency of 1600 per second, and employs a  $10^\circ \times 10^\circ$  134mm f1.8 infrared lens system. Color imaging is recorded on FM tape and real time images are displayed on a color cathode ray tube. A temperature controlled thermal source is used to set the temperature reference for the 10 scale color display. Temperature range settings allow a minimum detectable temperature difference of less than  $0.2^\circ\text{C}$  at  $30^\circ\text{C}$  for object temperature to be obtained.

## RESULTS AND DISCUSSION

### Postlaunch Effluent Calculations

Effluent dispersion calculations were made after the launch using the launch-time meteorological conditions so that the model could be compared with the effluent measurements and the observed cloud behavior. These effluent calculations were performed by MSFC using the multilayer diffusion model of reference 3. Details concerning the application of the model and the assumptions used in post launch predictions for the February 11, 1974, launch are being published by MSFC as a separate NASA report. The meteorological conditions used in the post launch analysis are based on T-38 minute rawinsonde sounding and T-zero thermodynamic and kinematic tower data. Figures 7, 8, 9, and 10 summarize the post launch calculations. Figure 7 shows the T-38 minute rawinsonde data. Figure 8 shows the HCl isopleths of 0.1 ppm and 1 ppm. As shown in Figure 8, maximum HCl concentration was predicted to be 1.5 ppm at 10.9 kilometers from the pad. In addition, the cloud path is shown to be  $125.6^\circ$  from the pad with cloud stabilization occurring at approximately 4.5 km from the pad. Figure 9 shows the predicted stabilization altitude (cloud centroid) to be about 900 meters and the cloud to have stabilized at this altitude approximately 380 seconds after launch. Figure 10 shows the centerline ( $125.6^\circ$ ) HCl concentrations and dosages as a function of distance from cloud stabilization (4.5 km from pad). The  $\text{Al}_2\text{O}_3$ , CO, and  $\text{CO}_2$  concentrations and dosages can be obtained from the HCl data of figure 10 by multiplying by the appropriate constants (Ref. 1) given in table VI.

### Effluent Measurements

Throughout the monitoring program, appropriate background sampling was conducted to define the ambient particle loading and hydrogen chloride concentration in the AFETR area. Background particle sampling occurred at T-7 days and T-6 days at a location of 12 km from LC-11 on an azimuth of  $177^\circ$ . This location was selected as it is representative of the majority of potential instrument sites at KSC. Six nuclepore samples, each of 2 hour duration, were taken during the background sampling period. In addition, three nuclepore filters were loaded into filter holders and then unloaded to determine handling effects. Each of these nine samples was weighed and then

subjected to neutron activation analysis. Table VII shows the results of these analyses. The  $24 \mu\text{gm}/\text{m}^3$  ambient air particle loading is similar to that reported during earlier launch monitorings at AFETR (Ref. 8). Ambient background sampling for the gas species (HCl, CO, and  $\text{CO}_2$ ) was conducted from T-30 minutes to launch time. HCl and CO concentrations were always below the detection limit of the instrumentation, being less than 0.05 ppm HCl and 0.5 ppm CO.  $\text{CO}_2$  concentrations ranged from about 310 to 340 ppm and was typical of expected ambient variations.

As already shown in figure 5, primary sites 1 through 4 located on the seacraft did not intersect the launch effluent cloud. The actual trajectory of the cloud was 25 to 30 degrees south of the southern most seacraft position. Post launch analysis of the data from these sites showed no evidence of launch effluents. In addition, some measurements were negated due to the rough seas and resulting sea spray. Primary site 5, located for background sampling gave data identical to that already discussed. Neutron activation analysis was not performed on the nuclepore samples at P-1 through P-5.

Table VIII shows nuclepore data from the other 19 sites. All nuclepore filters were weighed before and after launch in a class 100 clean room and then only after the sample had equilibrated to the clean room environment. Column 5 is the uncorrected weight gain of the filter (post launch weight minus prelaunch weight). Column 6 is the corrected weight gain obtained from column 5 by correcting for handling and normal ambient background effects. Equation 1 is used to calculate corrected weight gain, where  $W_H$  and  $\chi_A$  were taken to be  $69 \mu\text{gm}$  and  $24 \mu\text{gm}/\text{m}^3$ , respectively.

$$W_c = (W_s - W_H) - \chi_A F t \quad (1)$$

Where:

$W_c$  = corrected weight gain,  $\mu\text{gm}$

$W_s$  = uncorrected sample weight gain,  $\mu\text{gm}$

$W_H$  = handling effects correction factor,  $\mu\text{gm}$

$\chi_A$  = normal ambient particle concentration,  $\mu\text{gm}/\text{m}^3$

$F$  = sample flow rate,  $\text{m}^3/\text{min}$ .

$t$  = sample time, min.

Of the corrected weight gains in table VIII only those above the one-sigma deviation (Table VII) of the normal ambient background and handling are considered statistically significant.



Table IX and figure 11 summarize the statistically significant nuclepore data and the other effluent data at these sites. The nuclepore data in the table is shown as particle dosage, a term compatible with the diffusion model output. Equation 2 is used to calculate particle dosage.

$$D_c = (W_c \times 10^{-3})/F \quad (2)$$

where:

$D_c$  = corrected particle dosage,  $\text{mgm-sec/m}^3$

$W_c$  = corrected weight gain (Table VIII),  $\mu\text{gm}$

$F$  = sample flow rate,  $\text{m}^3/\text{sec}$

$10^{-3}$  = conversion factor,  $\text{mgm}/\mu\text{gm}$

The instrument activation and sample times shown in table VIII apply to both bubblers and nuclepores. Bubbler analysis was by a coulometric technique resulting in a detection limit of 80 ppm-sec (0.2 ng/ $\mu\text{l}$  chloride for the bubbler system used). Data from the high volume samplers at site CC, DD, FF, and MM and the Andersen sampler at MM are not shown in table IX, as an insufficient sample was obtained for analysis. As shown in the figure, the data shows some consistency in identifying above ambient effluent loading in the surface wind and cloud trajectory direction from the pad ( $120^\circ$ - $160^\circ$ ). In addition potential data discrepancies (see Table IX) occur at S-3, DD, and FF; in that, from model calculations and past monitoring experience, sites showing positive bubbler results should also show above ambient nuclepore data. To gain additional insight into the data of table IX, the nuclepore samples with above ambient weight gains were analyzed by neutron activation to determine the percentage of the total weight gain that is attributed to that element (aluminum) known to be present in a valid particulate sample of the launch cloud. The results are shown in table X. Nuclepore samplings at S-9 and S-14 showed no aluminum above normal ambient background and handling effects and thus the weight gains observed for those samples are not attributed to the launch vehicle exhaust. In addition, the data of table X shows that only the nuclepore sample at site MM (taken on launch complex) has a sizeable aluminum weight gain as compared to the total nuclepore weight gain. It is concluded from table X, that only that nuclepore sample at MM is a verified launch exhaust sampling. It should be noted that the aluminum weight gains at sites S-5, S-13, S-15, and CC were above ambient and handling effects and under conditions of supporting gas or additional particle data at the site, might be considered significant.

To gain further insight into the bubbler data at sites S-3, DD, and FF, these bubbler samples were subjected to sodium analyses, to determine if the observed chloride concentrations could be accounted for by sea salt contamination. The sodium analysis was unable to answer the question as control bubbler samples (distilled water) showed large sodium concentrations. Sodium

is probably a contaminate in the bubbler glass. The lack of particle data at sites S-3, DD, and FF makes the HCl data at these sites suspect. Additional information for further data interpretation is not available; however, the lack of a pH paper color changes at S-3 suggests that the observed chloride concentration at the site is probably chloride contamination. Past experience has shown that approximately 2 to 5 percent of the bubblers used in a study like this become contaminated in handling. The pH paper color change at sites DD and FF suggest that the bubbler data at these sites were the result of HCl from the launch. However, due to the close proximity of these sites to the pad, the surface wind direction, and the measured cloud trajectory, these samplings may be the launch cloud or pad debris carried by the surface wind. The data of figure 11 and table IX is of little significance in assessing the model for three basic reasons:

1. All data was obtained prior to cloud stabilization and additional data after stabilization was not obtained. (Model is not designed for effluent predictions prior to cloud stabilization.)
2. Effluent results obtained were measured with dosage type instruments, not selective to the species being detected, and in many cases measured dosages were marginal.
3. Dosage type data obtained had inconsistencies which could not be resolved.

In summarizing the effluent data obtained during the February 1974 Titan launch, it is concluded that no significant gas or particulate measurements suitable for model comparison were obtained. Primary sites were unable to intersect the ground effluent cloud. Secondary site data was limited and that obtained was of low concentration and inconsistent. Several operational changes are apparent from the monitoring mission.

1. Primary sites should be increased to at least eight, with provisions for deploying all eight at sea. This allows for a larger sampling grid work with a higher probability of being able to adjust plus time to the cloud trajectory. In addition, in cases where the cloud trajectory is predicted to lie in the region of the launch vehicle flight path, four seacraft can be located on each side of the seacraft prohibited zone, thus assuring adequate instrument siting both north and south of this zone.
2. Provisions should be made to reposition seacraft in the plus count based on real time metric track (see next section) of the ground cloud.
3. Seacraft must be larger and capable of operating and maintaining 10-12 knots in rough seas (4 ft. seas). Seacraft of 30 to 40 foot in length do not provide adequate sampling platforms in rough seas.
4. Tighter controls are necessary on the secondary instrumentation to minimize handling contamination. For instance, solenoid shutters on nucleopore filters which open and close automatically during the sampling operation.

5. The problems associated with dosage, non-selective instrumentation are well illustrated in this monitoring effort and the importance of using real time, more selective instrumentation in conjunction with the dosage (secondary instrumentation) type instrument is reinforced.

#### Optical Measurements of Cloud Behavior

The metric tracking cameras optically tracked the exhaust cloud for approximately 50 minutes. Figure 12 shows the measured rise of the cloud to its stabilization altitude. The error bars are one sigma deviations determined from data taken with the three metric tracking units. The cloud stabilized at an altitude of 1100 meters at T+5 minutes, and continued drifting downwind at the stabilization altitude. As shown in figure 12 a mild temperature inversion existed at about 1100 meters. The ground track of the cloud is shown in figure 13. A comparison of the data of figures 12 and 13 with that previously discussed from the T-zero model is shown in table XI. As can be seen the comparison is quite good with only a 100 meter and  $10^\circ$  discrepancy in stabilization altitude and cloud path, respectively. Figure 14 summarizes the measured cloud rise data for two Titan launches. During the first 4 minutes following the launch, both clouds rise at nearly 4.8 meters/second, apparently independent of the existing wind field and vertical thermodynamic structure of the lower atmosphere. Following the initial rise, the clouds then stabilize at an altitude that is strictly dependent on the vertical temperature and wind field that exists from the surface upwards for the first few kilometers.

Shown in figure 15 are visible spectrum photographs taken from UCS 9 (11.5 km,  $327^\circ$  from LC-41) at the times indicated. These visible photographs offer a means for determining the cloud volume history during its rise and growth following ignition. The technique used is that of dividing the cloud into small area elements. Using similar images from another camera site at right angle (ideal case) to the original site allows volume elements to be calculated and summed to give the total cloud volume. The technique is an approximation because of the irregularities in the cloud shape, some of which cannot be resolved by the method. A check can be made however, if a third camera site can furnish images of the cloud and thus allow a second and possibly a third volume determination to be made. Figure 16 is a plot of the cloud volume as a function of time for the February 11, 1974, Titan ground cloud. The upper curve was obtained from the photographic data of UCS 9 and 26. The lower curve, from UCS 2 and 26. This data, as well as similar data to be obtained at future Titan launches, can be used to evaluate the model assumptions of cloud volume at stabilization and volume expansion rate after cloud stabilization.

In addition to the metric tracking and visible photographic data at UCS 9, infrared cloud imaging data was also obtained. Figure 17 shows at various times after launch, a comparison of visible and infrared images. As shown the image comparison is quite good with improved cloud definition being apparent from the infrared data at the longer times after launch. Since UCS 9 was almost  $180^\circ$  up-range of the cloud trajectory, the infrared data was used to calculate the crosswind growth of the cloud. Figure 18 shows the results, where the crosswind parameter is the maximum horizontal dimension of the cloud.

Corresponding crosswind dimensions obtained from visible photographs at UCS 9 are also shown for reference at the earlier times after launch. As shown in the figure, the visible and infrared data compared well and the crosswind cloud growth appears to be such that the crosswind dimension subtends a 5 degree angle. The data of figures 17 and 18 show that infrared imaging is a viable technique for measuring such cloud parameters as cloud rise, growth, and track; and can provide better cloud definition than visible photographs.

The infrared data from UCS 9 was analyzed to determine the cloud temperature as a function of time after launch. A very complex and dynamic cloud temperature structure was found to exist. Figure 19 shows the extremes of the cloud temperature from T-zero to T+25 minutes. The temperatures are temperature differentials as referenced to ambient temperature. The data of figure 19 assumes the cloud emits radiation as a black body. Below ambient cloud temperatures although not physically occurring within the cloud, are the result of this black body assumption. Temperature resolution of the infrared system for those measurements was 0.5°C increments. Although, the cloud temperature structure is complex and cannot be completely understood from this set of measurements, the cloud appears to have sufficient temperature change from the ambient to consider an infrared experiment to identify HCl. Such an experiment would consist of two infrared imaging systems, one of which measures all incoming radiation (background and HCl) and the second of which is filtered to remove incoming HCl radiation.

In summary, optical measurements of cloud rise, growth, stabilization and path agreed reasonably well with that predicted by the T-zero model calculations. In addition, the first known cloud volume and crosswind growth measurements of a full scale Titan cloud were made. These measurements along with future measurements of the same type will provide a much needed check on the cloud parameters used in the MSFC model. Infrared imaging was able to monitor exhaust cloud temperatures showing a complex cloud temperature profile.

#### CONCLUDING REMARKS

In summarizing the effluent data obtained during the February 1974 Titan launch, it is concluded that no significant gas or particulate measurements suitable for model comparison were obtained. As a result of the changing meteorology, the rough sea conditions, and the range safety constraints on seacraft operations, the primary instruments located on the seacraft did not intersect the Titan launch cloud. Those effluent measurements obtained were limited to land sites within 3 kilometers of the launch pad. Data from these sites were limited and that obtained were of low concentrations and inconsistent. The inconsistencies in the data is attributed to the non-selective, dosage type instruments used at these locations and the low effluent concentrations occurring prior to cloud stabilization. (The exhaust cloud stabilized 4.5 kilometers from the launch pad.)

Optical measurements of cloud rise, stabilization, and path agreed reasonably well with that predicted by the T-zero model calculations (post

launch calculations). In addition, the first known cloud volume and cross-wind growth measurements of a full scale Titan cloud were made. These measurements along with future measurements of the same type will provide a much needed check on the cloud parameters used in the MSFC model. Infrared imaging techniques were able to track the cloud and able to monitor exhaust cloud temperatures showing a complex cloud temperature profile.

As a result of the sampling mission, several operational changes are recommended. These are briefly summarized below:

1. Primary sites should be increased to at least eight with provisions for deploying all eight at sea.
2. Plans should be made to reposition seacraft in the plus count based on real time metric cloud track data.
3. Larger seacraft (greater than 12 meters in length) capable of speeds of 5 to 6 meters/second (10-12 knots) in rough seas are required.
4. Contamination of secondary instrument (dosage instrument) sets must be further reduced.

#### REFERENCES

1. Stephens, J. Briscoe: Atmospheric Diffusion Predictions for the Exhaust Effluents from the Launch of a Titan III-C, December 13, 1973. NASA TM-64925, September 1974.
2. Wagner, H. Scott: Measurement of Solid Rocket Motor Effluents in the Atmosphere. Prepared for Sixth Conference on Environmental Toxicology, October 21-23, 1975.
3. Dumbauld, R. K.; Bjorklund, J. R.; and Bowers, J. F.: NASA/MSFC Multi-layer Diffusion Models and Computer Program for Operational Prediction of Toxic Fuel Hazard NASA CR-129006, 1973.
4. Gregory, Gerald L.; Hudgins, Charles H.; and Emerson, Burt R., Jr.: Evaluation of a Chemiluminescent Hydrogen Chloride and a NDIR Carbon Monoxide Detector for Environmental Monitoring. 1974 JANNAF Propulsion Meeting, Volume I, Part II, CPIA Publ. 260 (Contract N00017-72-C-4401), Appl. Phys. Lab., John Hopkins Univ., Dec. 1974, pp. 681-704.
5. Stedman, D. H. and Kok, G. L.: Chemiluminescent Measurement of Atmospheric Acid. Final report NASA Grant No. NGR23-005-599, Univ. Michigan, College of Engineering, May 1974.
6. Reyes, Robert J.; Miller, Richard L.; and Beatty, David C.: Monitoring of HCl from Solid Propellant Launch Vehicles. 1974 JANNAF Propulsion Meeting, Volume I, Part II, CPIA Publ. 260 (Contract N00017-72-C-4401), Appl. Phys. Lab., Johns Hopkins Univ., Dec. 1974, pp. 705-722.
7. Hulten, William C.; Storey, Richard W.; Gregory, Gerald L.; Woods, David C.; and Harris, Franklin S., Jr.: Effluent Sampling of Scout "D" and Delta Launch Vehicle Exhausts. NASA TMX-2987, 1974.
8. Gregory, Gerald L. and Storey, Richard W., Jr.: Effluent Sampling of Titan III-C Vehicle Exhaust. NASA TMX-3228, 1975.

TABLE I: TITAN SRM EXHAUST COMPOSITION

Constituent	Mass Fraction	
	Exit Plume <sup>a</sup>	Plume at 1 Kilometer <sup>b</sup>
Aluminum oxide ( $\text{Al}_2\text{O}_3$ )	0.304	0.002
Carbon monoxide (CO)	0.279	— <sup>c,d</sup>
Hydrogen Chloride (HCl)	0.210	0.001
Nitrogen ( $\text{N}_2$ )	0.084	0.784
Water Vapor ( $\text{H}_2\text{O}$ )	0.067	0.002
Carbon dioxide ( $\text{CO}_2$ )	0.029	0.002
Hydrogen ( $\text{H}_2$ )	0.025	— <sup>d</sup>
Oxygen ( $\text{O}_2$ )	— <sup>d</sup>	0.208
Others	0.002	0.001

a - reference 1

b - reference 2

c - majority of CO converted to  $\text{CO}_2$  in plume afterburning

d - less than 0.001

TABLE II: SUMMARY OF MSFC EFFLUENT DISPERSION PREDICTIONS, MINUS COUNT

T-minus time, hours	Cloud stabilization altitude, meters	Cloud path from LC-41 degrees, true	Peak HCl concentration, ppm	Location of peak from LC-41, Kilometers
T - 72	610	16.9	0.4	7.6
T - 48	NA*	196.2	0.9	8.4
T - 24	690	143.5	0.5	7.3
T - 12	750	128.8	1.0	12.3
T - 8	540	124.2	2.6	5.2
T - 6	700	85.5	0.6	7.7
T - 2	640	110.3	2.1	9.9

\* not available

REPRODUCIBILITY OF THE  
ORIGINAL PAGE IS POOR



TABLE III: MEASUREMENT SITE LOCATION RELATIVE TO LAUNCH COMPLEX 41

Site designation	Azimuth, degrees, true	Distance from LC-41, Kilometers
P - 1 <sup>a</sup>	75.5	12.0
P - 2 <sup>a</sup>	75.5	14.6
P - 3 <sup>a</sup>	83.5	14.8
P - 4 <sup>a</sup>	84.5	15.7
P - 5	283	2.6
S - 1	3.4	1.0
S - 2	7.6	0.9
S - 3	14.8	0.8
S - 4	21.8	0.7
S - 5	29.6	0.6
S - 6	40.6	0.6
S - 7	57.3	0.5
S - 8	72.7	0.5
S - 9	91.6	0.6
S - 10	101.3	0.6
S - 11	113.2	0.7
S - 12	121.5	0.8
S - 13	126.9	0.9
S - 14	130.8	1.0
S - 15	133.9	1.1
CC	152	2.7
DD	136	1.3
FF	147.3	2.0
MM	90	0.1

a - seacraft position at lift-off - not sampling position

TABLE IV: EQUIPMENT SITE PLAN

Site designation	Instrument	Species
P - 1	Coulometer	HCl
	Chemiluminescent (I) <sup>a</sup>	HCl
	Bubbler	HCl
	pH paper	HCl
	Infrared detector	CO <sub>2</sub>
	DIF infrared detector	CO
	Mass monitor	particles
	Light photometer (Climet)	particles
	Andersen	particles
	nuclepore	particles
P - 2	Bubbler	HCl
	pH paper	HCl
	DIF infrared detector	CO
	Mass monitor	particles
	Light photometer (Climet)	particles
	Andersen	particles
	Nuclepore	particles
P - 3	Coulometer	HCl
	Chemiluminescent (II) <sup>b</sup>	HCl
	Bubbler	HCl
	pH paper	HCl
	Infrared detector	CO <sub>2</sub>
	DIF infrared detector	CO
	Mass monitor	particles
	Light photometer (Royco)	particles
	Andersen	particles
	Nuclepore	particles

TABLE IV: CONTINUED

Site designation	Instrument	Species
P - 4	Bubbler	HCl
	p H paper	HCl
	DIF infrared	CO
	Mass monitor	particles
	Andersen	particles
	Nuclepore	particles
P - 5	Bubbler	HCl
	pH paper	HCl
	DIF infrared	CO
	Mass monitor	particles
	Andersen	particles
	Nuclepore	particles
	Inertial impactor	particles
S - 1 to S - 15	Bubbler	HCl
	pH paper	HCl
	Nuclepore	particles
CC, DD, and FF	Bubbler	HCl
	pH paper	HCl
	Nuclepore	particles
	High volume	Particles
MM	pH paper	HCl
	Andersen	particles
	Nuclepore	particles
	High volume impactor	particles

a - chemiluminescent detector, type I - detects HCl directly

b - chemiluminescent detector, type II - reacts HCl with known quantity of  $\text{NH}_3$ , converts remaining  $\text{NH}_3$  to NO, and then detects NO by chemiluminescent principles

TABLE V: INSTRUMENT CAPABILITIES

## PART I - GAS INSTRUMENTS

Instrument/species	Range	Detection Limit	Response to 90-percent reading	Required Analysis
Chemiluminescent I/HCl (ref. 4)	0.05 to 50 ppm	0.05 ppm	1 to 5 sec	None
Chemiluminescent II <sup>a</sup> /HCl (ref. 5)	0.05 to 10 ppm	0.05 ppm	30 sec	None
Microcoulometer/HCl (ref. 6)	0.1 to 20 ppm	0.1 ppm	1 to 5 sec	None
Bubbler/HCl (ref. 7)	greater than 80 ppm-sec	80 ppm-sec	not applicable	Coulometric
pH paper/HCl (ref. 7)	qualitative	1 ppm	not applicable	None
Infrared detector <sup>a</sup> /CO <sub>2</sub>	1 to 50 ppm above ambient	1 ppm above ambient	2.5 sec	None
DIF infrared/CO (ref. 4)	0.5 to 200 ppm	0.5 ppm	28 sec	None

## PART II - PARTICLE INSTRUMENTS

Instrument	Range ( $\mu$ m Diameter)	Detection Limit	Response to 90-percent reading	Required Analysis
Royco Photometer <sup>a</sup> (ref. 7)	0.5 to 6.5	1 particle	1 msec	Computer Processing
Climet Photometer <sup>a</sup> (ref. 7)	0.3 to 10.0	1 particle	1 msec	Computer Processing
Mass Monitor <sup>a</sup> (ref. 7)	0.1 to 20.0	10 $\mu$ g/m <sup>3</sup>	5 sec	None
Nucleopore Filter <sup>a</sup> (ref. 7)	>0.01	10 $\mu$ g	not applicable	Gravimetric NAA <sup>b</sup>
High Volume Cascade Impactor <sup>a</sup> (ref. 7)	>0.01	200 $\mu$ g	Not applicable	Gravimetric NAA
Andersen Cascade Impactor <sup>a</sup> (ref. 7)	0.43 to 11.0	50 $\mu$ g	Not applicable	Gravimetric NAA
Lundgren Cascade Impactor <sup>a</sup> (ref. 7)	0.5 to 14.0	50 $\mu$ g	Not applicable	Gravimetric NAA

a - Instrument Specifications based on manufacturer's data.

b - Neutron Activation Analysis

REPRODUCIBILITY OF THE  
ORIGINAL PAGE IS 100%

TABLE VI: EFFLUENT CONVERSION FACTORS

Species	Conversion Factor
$\text{Al}_2\text{O}_3$	2.22
CO	1.73
$\text{CO}_2$	0.11

Example:

$\text{Al}_2\text{O}_3$  concentration (or dosage) = 2.22 HCl concentration (or dosage)

CO,  $\text{CO}_2$ , HCl concentration in ppm

$\text{Al}_2\text{O}_3$  concentration in  $\text{mgm}/\text{m}^3$

CO,  $\text{CO}_2$ , HCl dosage in ppm-sec

$\text{Al}_2\text{O}_3$  dosage in  $\text{mgm-sec}/\text{m}^3$

TABLE VII: PARTICULATE BACKGROUND RESULTS

Source	Total		Aluminum		Chlorine	
	Mean	$\sigma$	Mean	$\sigma$	Mean	$\sigma$
Handling Effects <sup>a</sup> ( $\mu\text{gm}$ )	69	31	0.10	0.07	0.95	0.16
Ambient Air <sup>b</sup> ( $\mu\text{gm}/\text{m}^3$ )	24	11	0.18	0.12	0.87	0.56

a - Based on 3 samples

b - Based on 6 samples

TABLE VIII: NUCLEPORE DATA-LAND SITES

Site No.	Instrument Activation Time	Instrument Sample Time (minutes)	Flow Rate (liters/minute)	Uncorrected Filter Weight Gain ( $\mu\text{gm}$ )	Corrected <sup>a</sup> Weight Gain ( $\mu\text{gm}$ )
S - 1	T - 0	62	24.6	103	-
S - 2	T - 0	10	25.2	119	43.8
S - 3	T - 0	10	25.6	54	-
S - 4	T - 0	10	27.9	59	-
S - 5	T - 0	10	28.0	200	124.3
S - 6	T - 0	10	27.1	96	20.6
S - 7	T - 0	10	28.2	117	41.2
S - 8	T - 0	10	27.7	114	38.2
S - 9	T - 0	10	28.1	197	121.4
S - 10	T - 0	10	26.7	123	47.5
S - 11	T - 0	10	28.7	119	43.1
S - 12	T - 0	10	26.0	92	16.6
S - 13	T - 0	10	26.7	218	142.6
S - 14	T - 0	10	28.3	193	117.2
S - 15	T - 0	10	25.8	172	96.8
CC	T - 1 min.	11	59.0	453	368.2
DD	T - 1 min.	11	49.5	65	-
FF	T - 1 min.	11	57.0	68	-
MM	T - 1 min.	11	53.9	873	789.6

a - Dash identifies filters that had no weight gain other than handling and ambient background

TABLE IX: EFFLUENT RESULTS, LAND SITES

Site No.	Bubbler (HCl) ppm-sec	pH Paper Color Change	Nuclepore Corrected Particle Dosage mgm-sec/m <sup>3</sup>
S - 1	<80	no	-
S - 2	<80	no	-
S - 3	150	no	-
S - 4	<80	no	-
S - 5	<80	no	266.4
S - 6	<80	no	-
S - 7	<80	no	-
S - 8	<80	no	-
S - 9	<80	no	259.2
S - 10	<80	no	-
S - 11	<80	no	-
S - 12	<80	no	-
S - 13	<80	no	320.4
S - 14	<80	no	248.4
S - 15	<80	no	225.0
CC	<80	no	374.4
DD	275	yes	-
FF	320	yes	-
MM	not appropriate	yes	879.0



TABLE X: PERCENTAGE OF ALUMINUM PRESENT IN NUCLEPORE SAMPLES

Site No.	Percentage of Filter Weight Attributed to Al
S - 5	0.23
S - 9	0
S - 13	0.37
S - 14	0
S - 15	0.13
CC	0.16
MM	10.82

TABLE XI: COMPARISON OF CLOUD PARAMETERS

Parameter	Measured	T-zero prediction
Stabilization altitude	1100 m	970 m
Time of stabilization	300-360 sec	379 sec
Trajectory	135°, true	125.6°, true

REPRODUCIBILITY OF THE  
ORIGINAL PAGE IS POOR

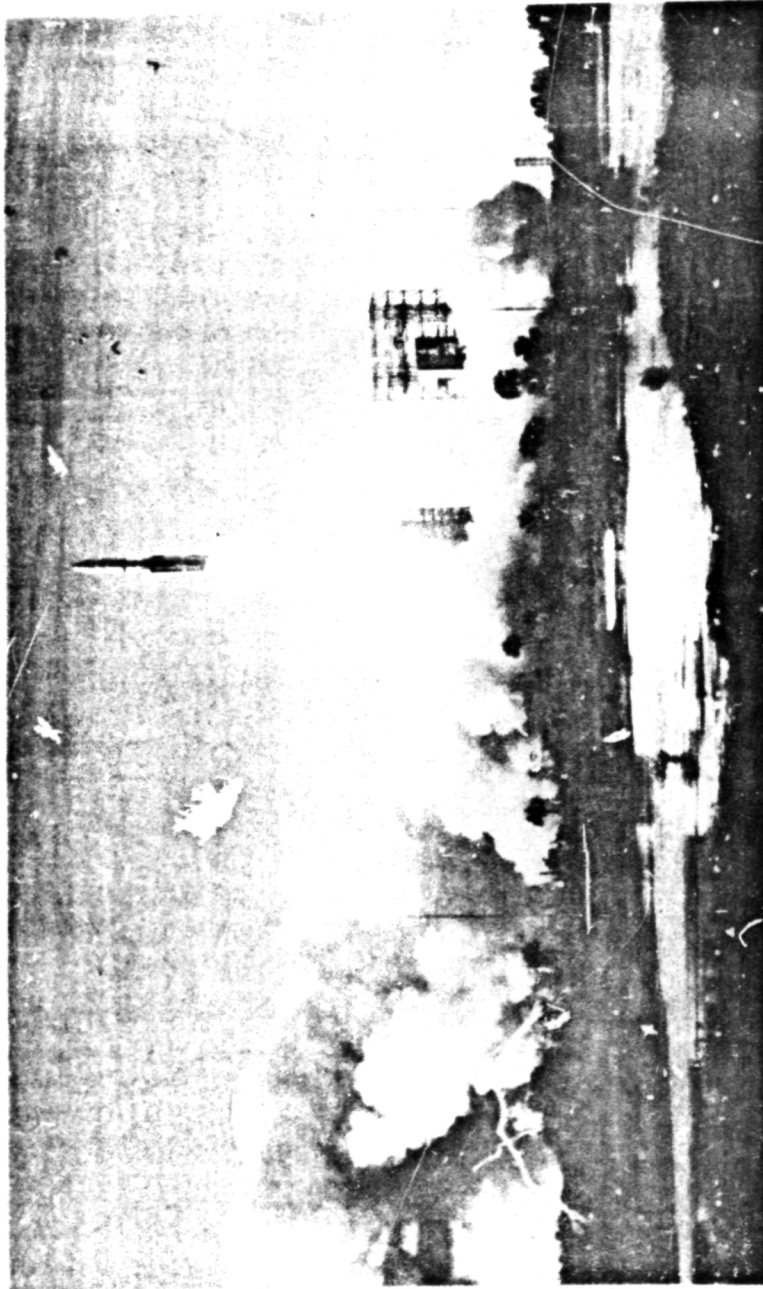


Figure 4. - February 11, 1974 River-Bent, 7 + 7 sec.

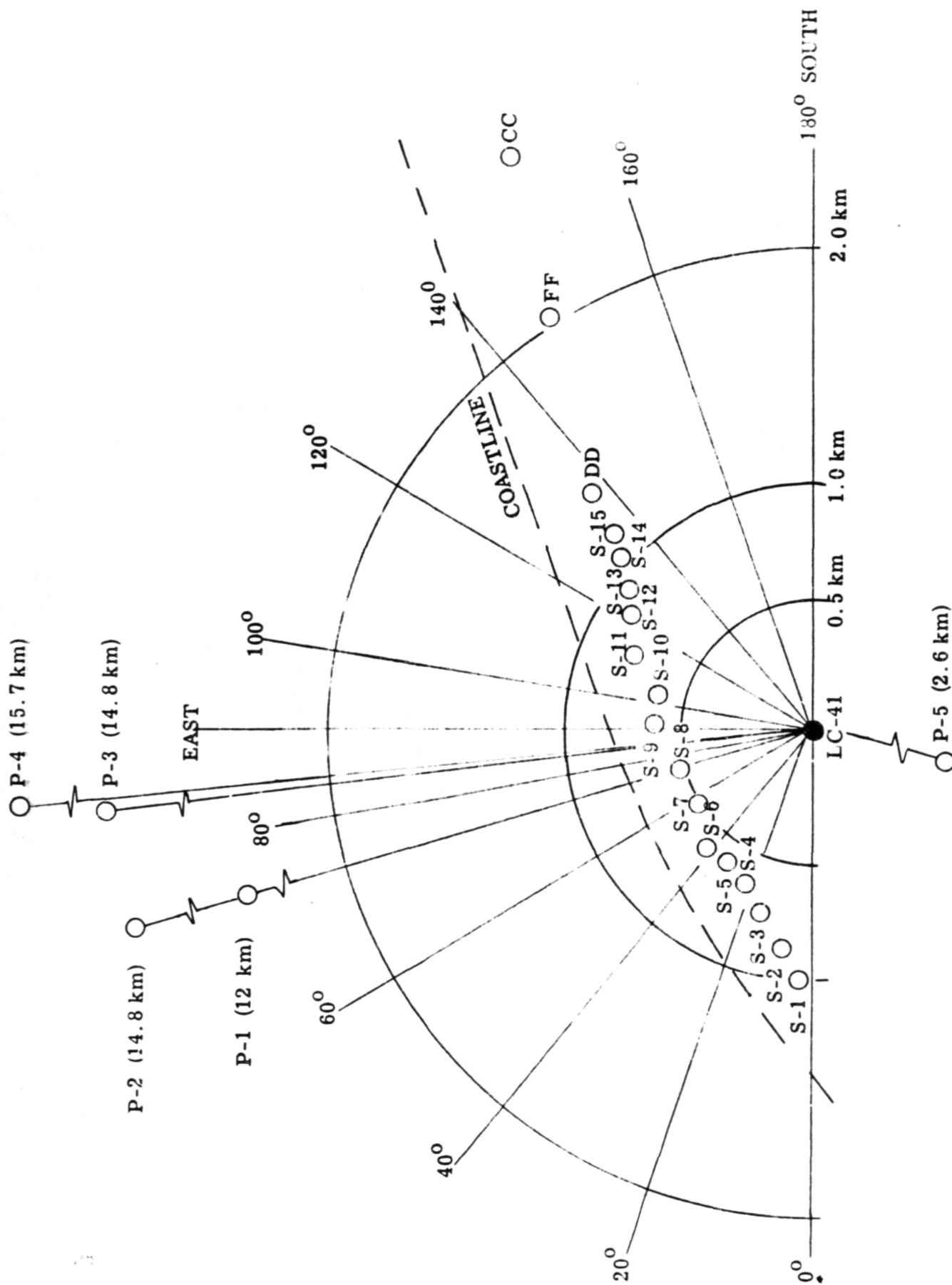


Figure 2. - Instrument site locations at lift-off.

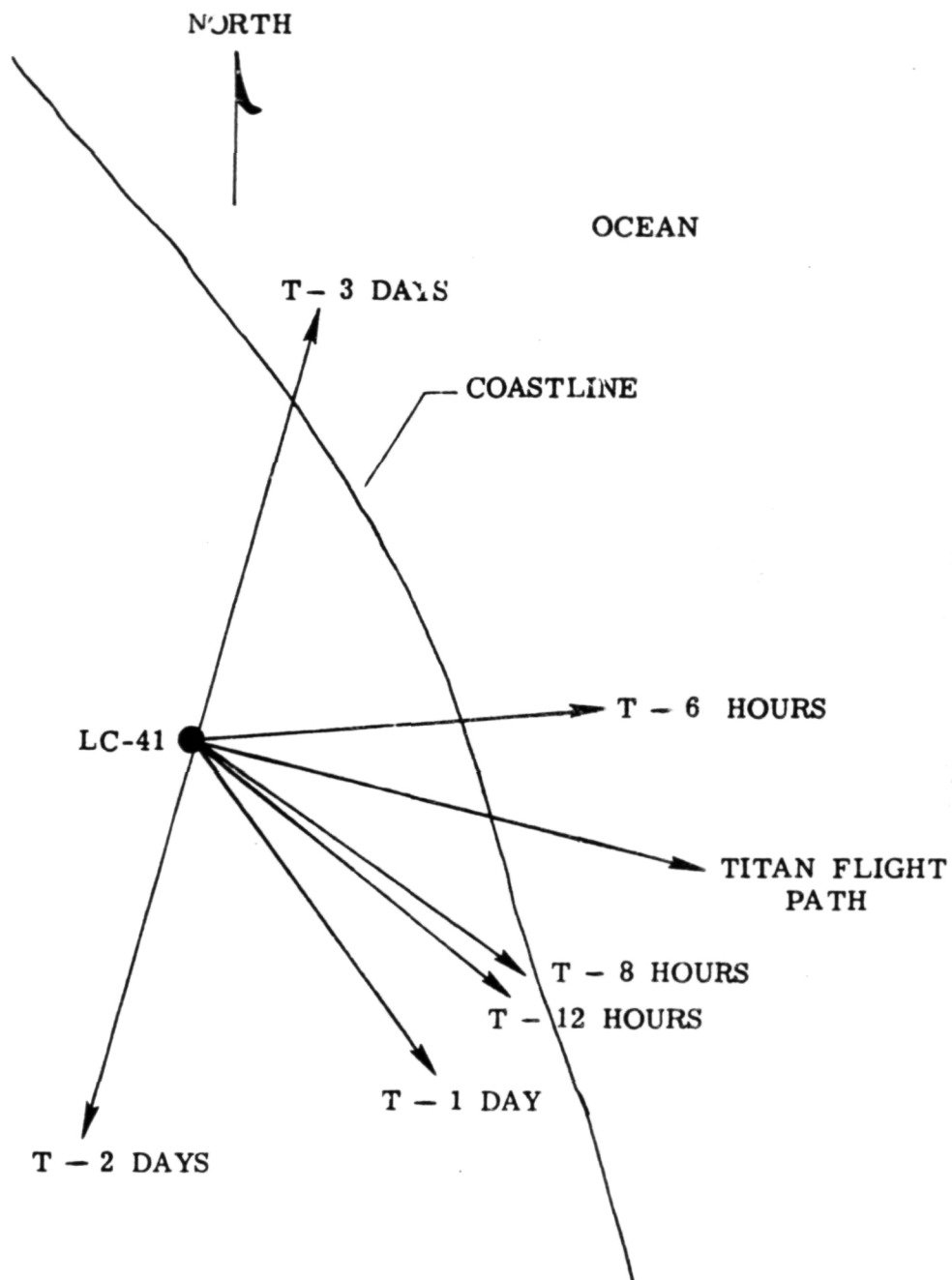


Figure 3. - Predicted cloud trajectory, T - 3 days to T - 6 hours.

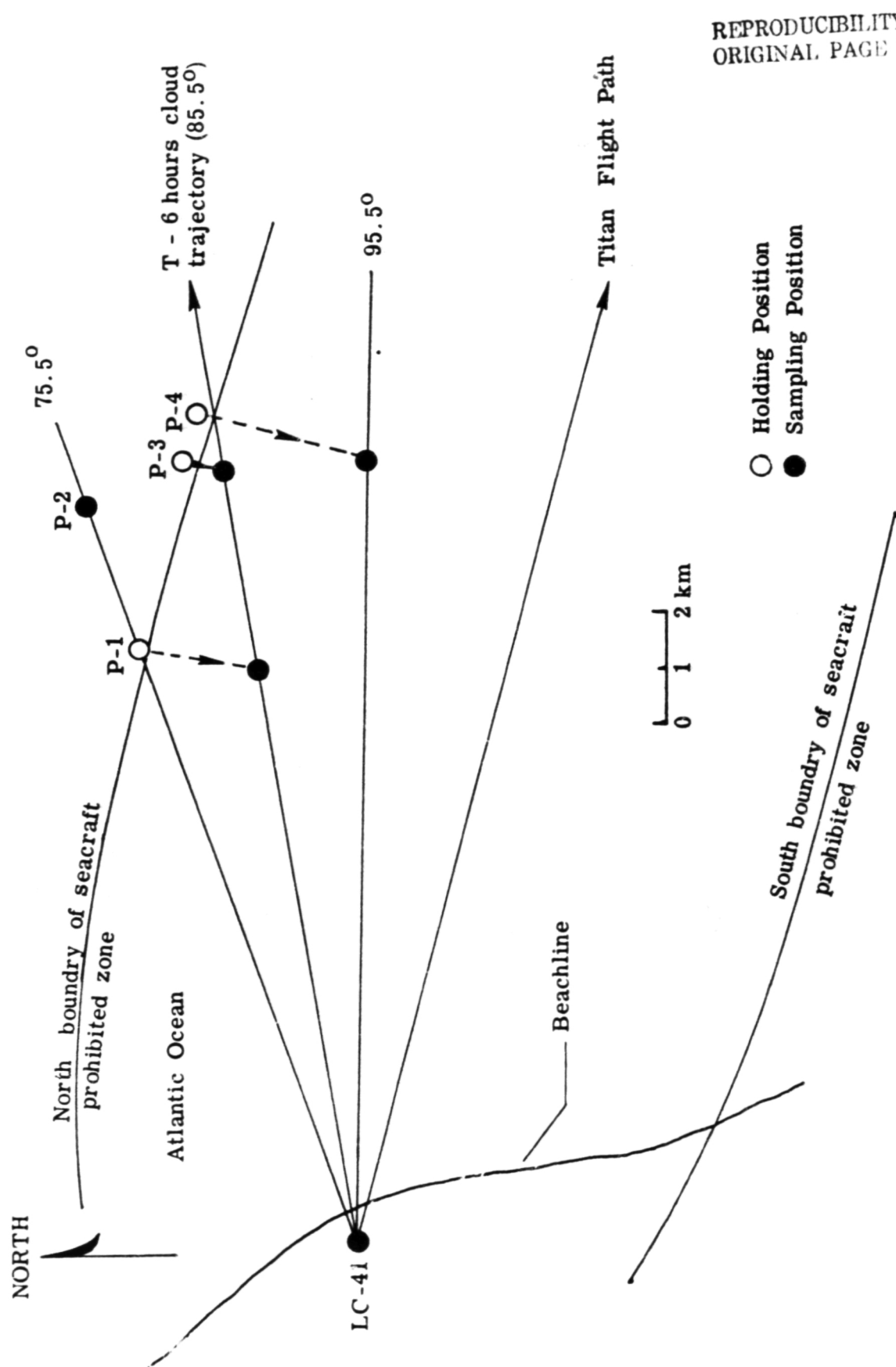


Figure 4. - Sampling plan for seacraft, based on T - 6 hour cloud trajectory.

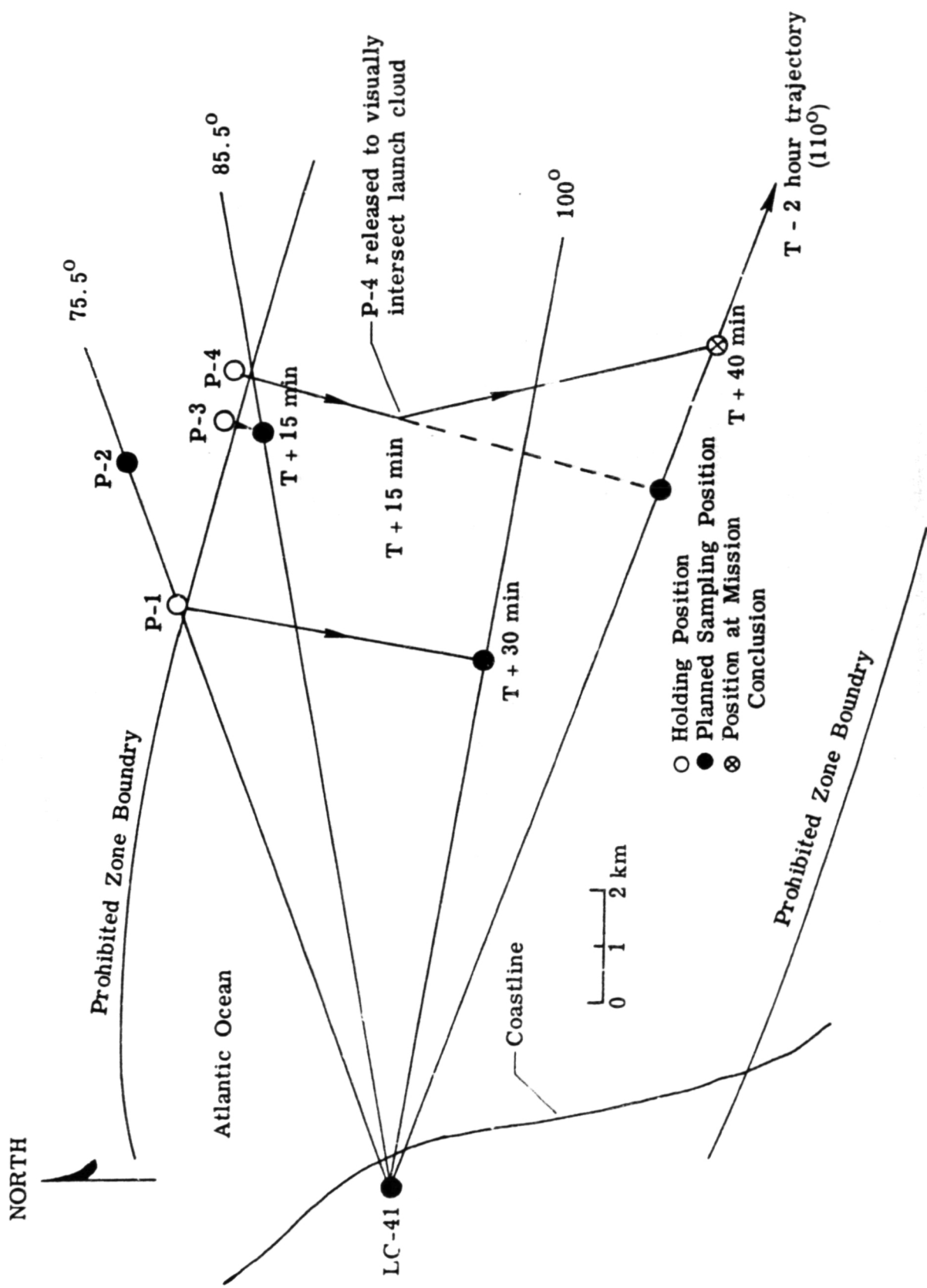


Figure 5. - Seacraft locations and paths.

REPRODUCIBILITY OF THE  
ORIGINAL PAGE IS POOR

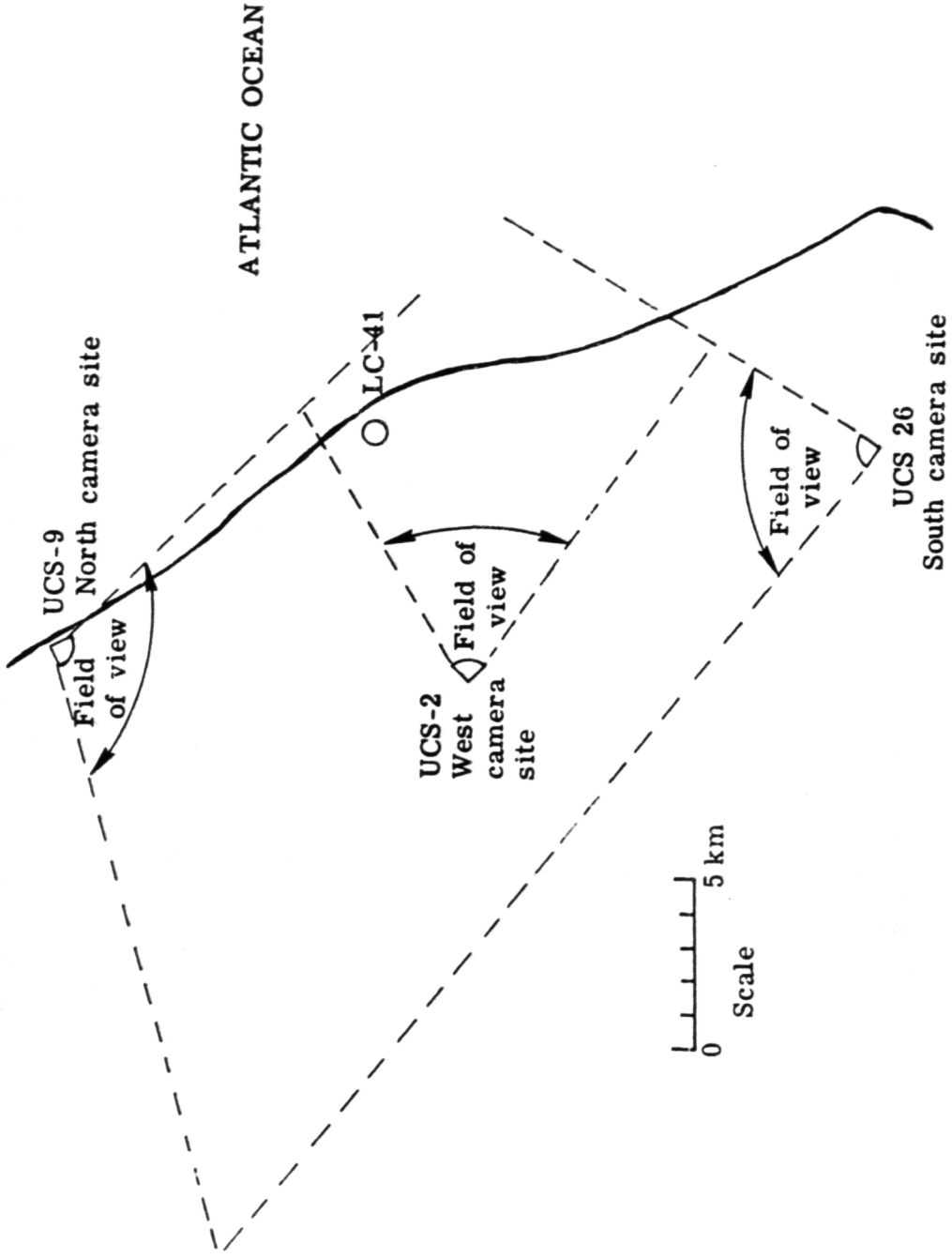


Figure 6. - Camera site plan.



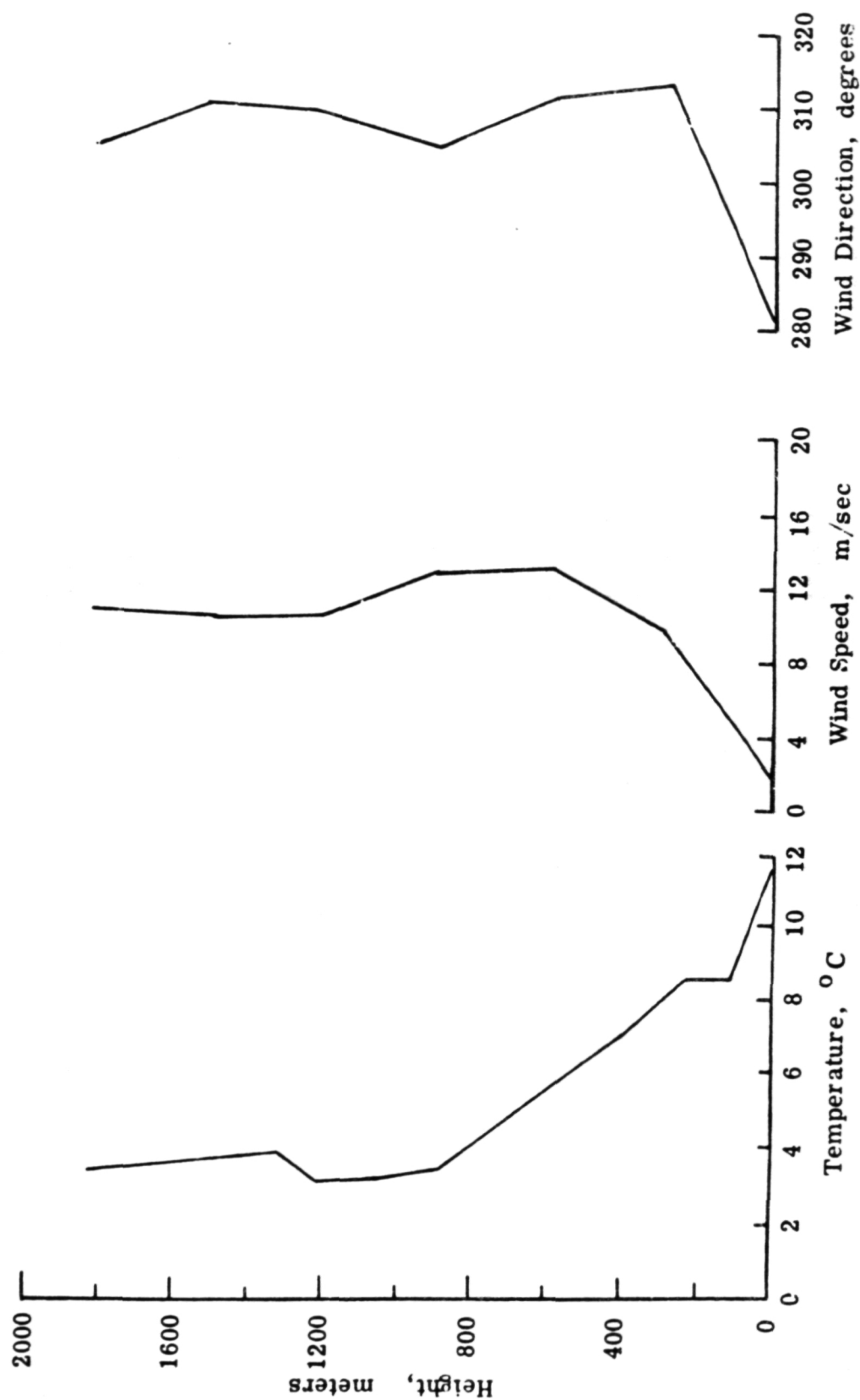


Figure 7. - Measured vertical profiles of temperature, wind speed, and wind direction, 0910 local time, February 11, 1974, KSC.

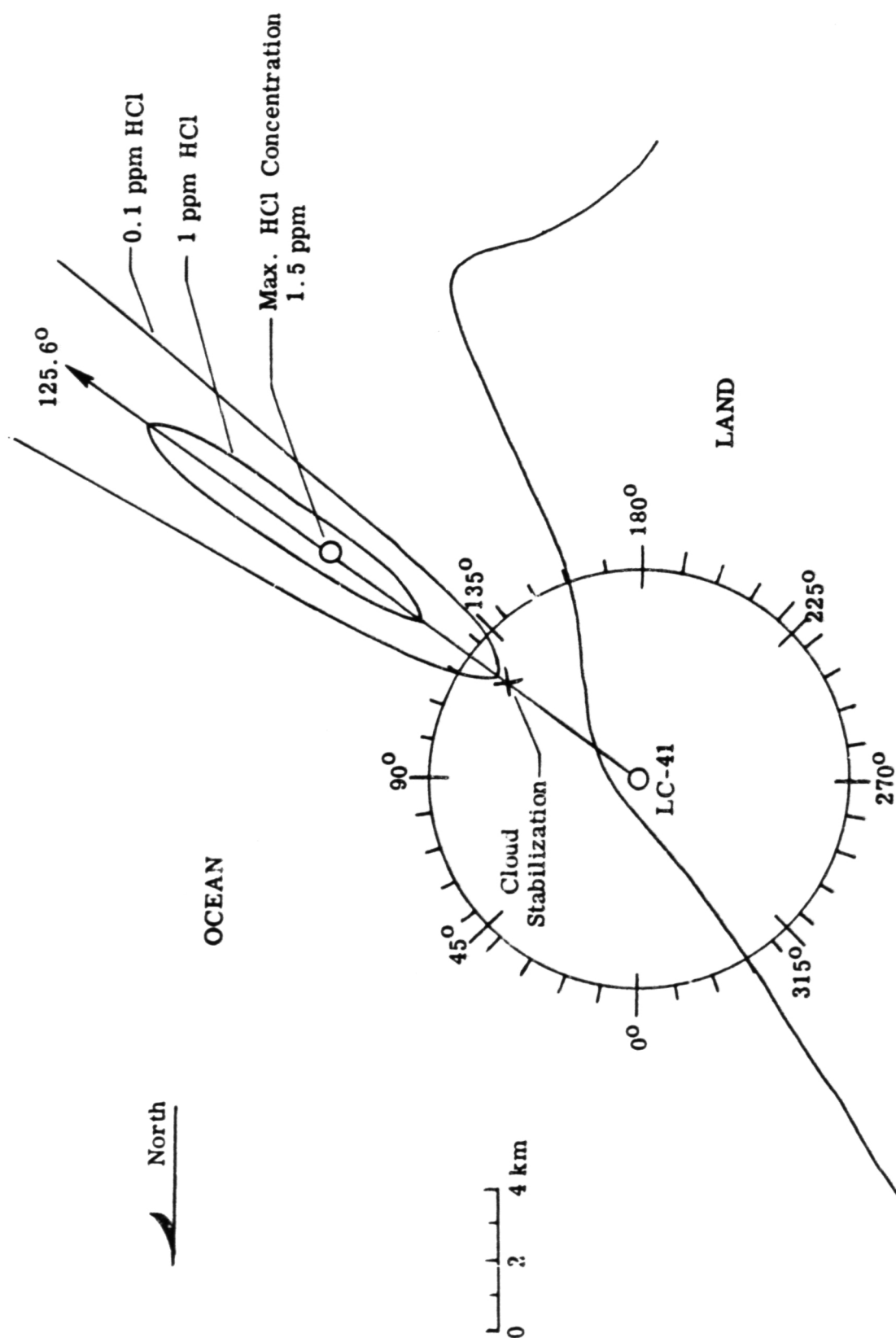


Figure 8. - T - zero model predictions, concentration isopleths.

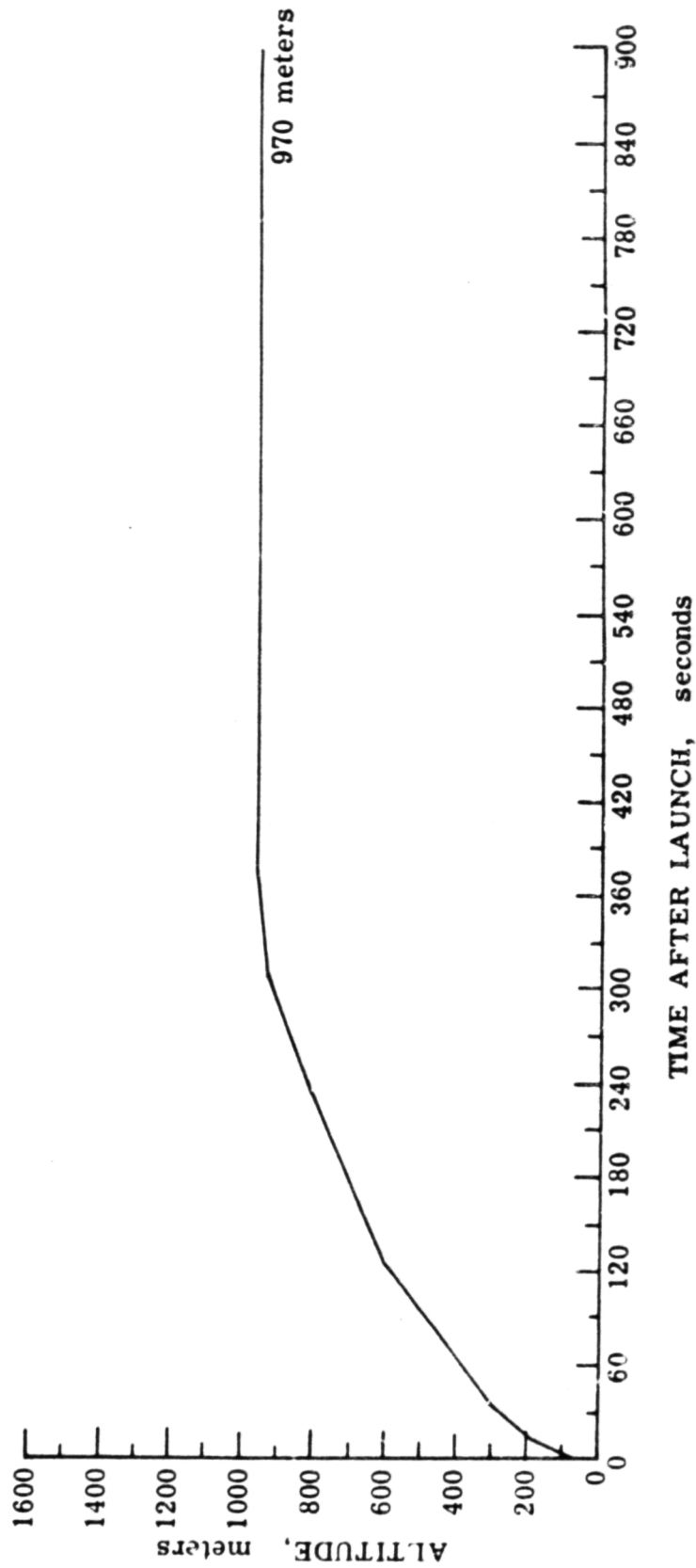
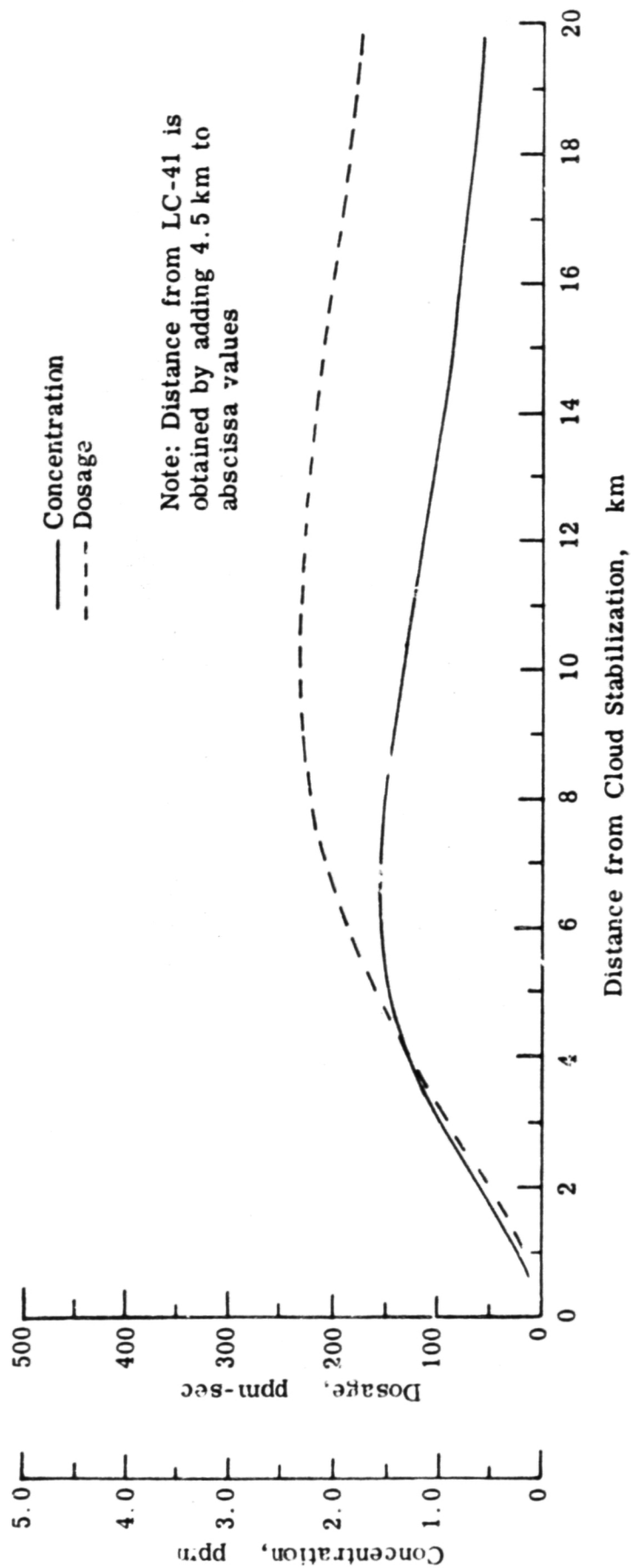


Figure 9. - T - zero model prediction, cloud stabilization.



REPRODUCIBILITY OF THE  
ORIGINAL PAGE IS POOR

Figure 10. - T - zero model prediction, centerline concentration and dosage.

- Denotes site locations where effluent measurements were normal ambient values
- Denotes site locations where above ambient effluent values were measured

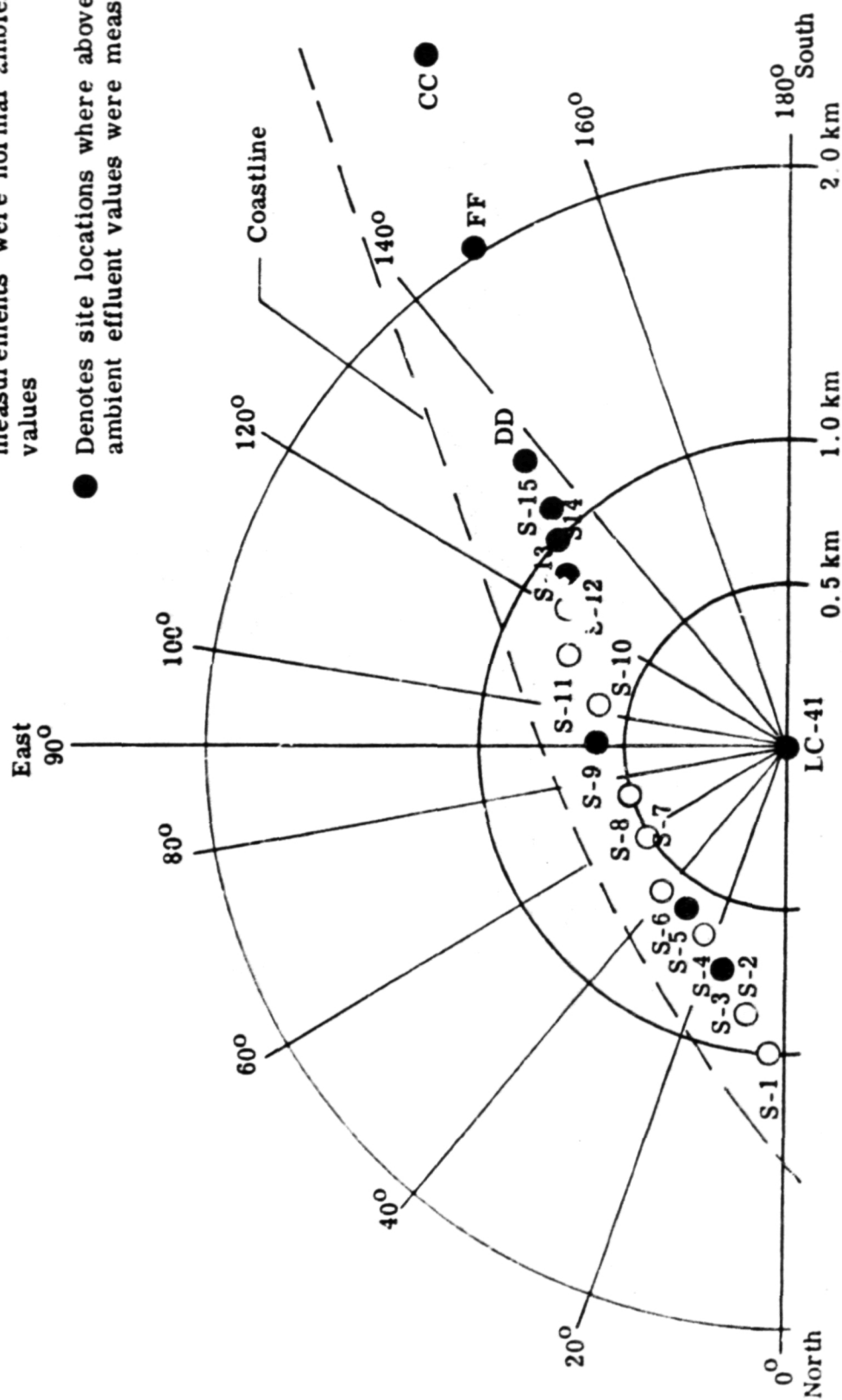


Figure 11. - Effluent measurement results.

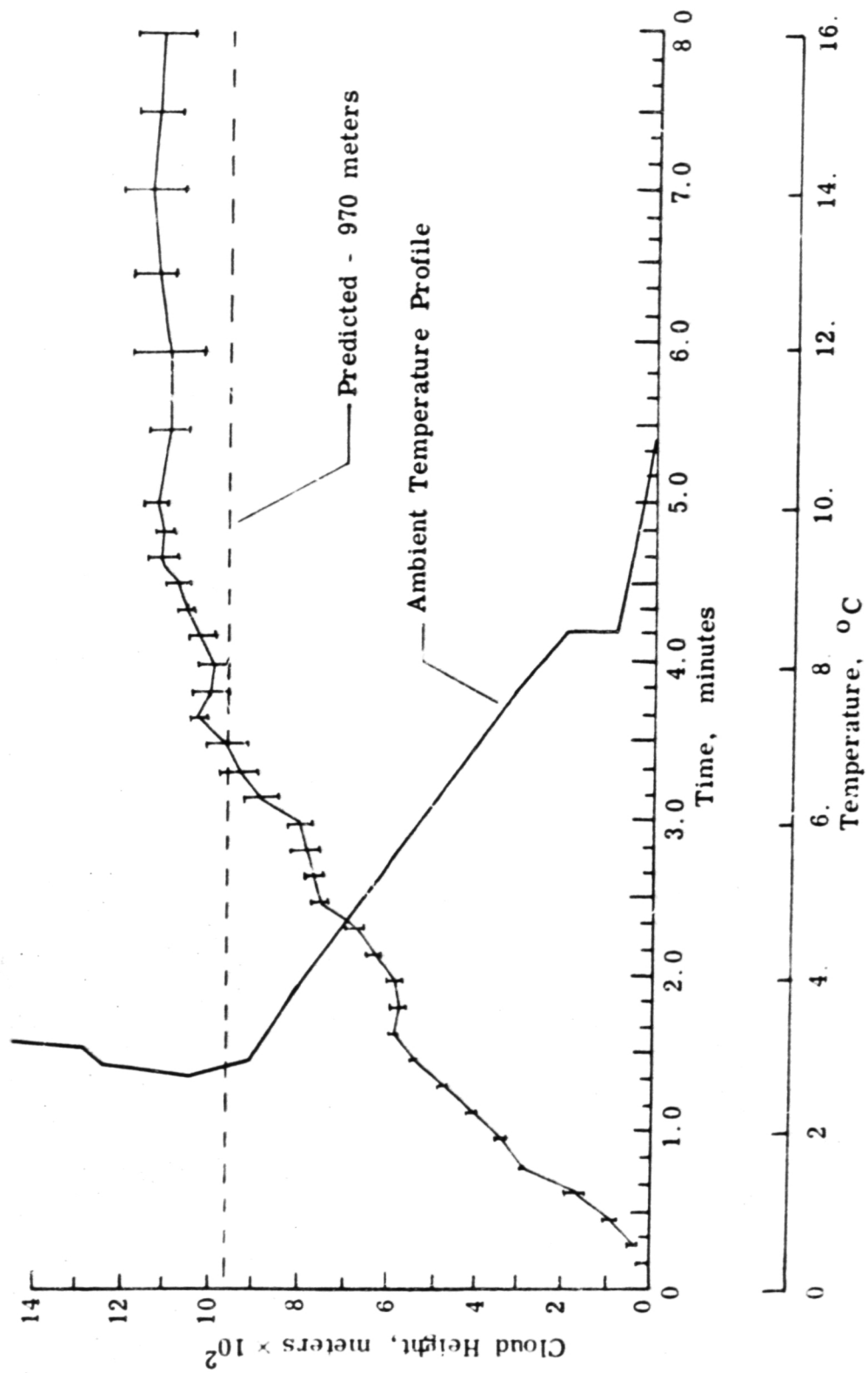


Figure 12. - Cloud rise and stabilization results.

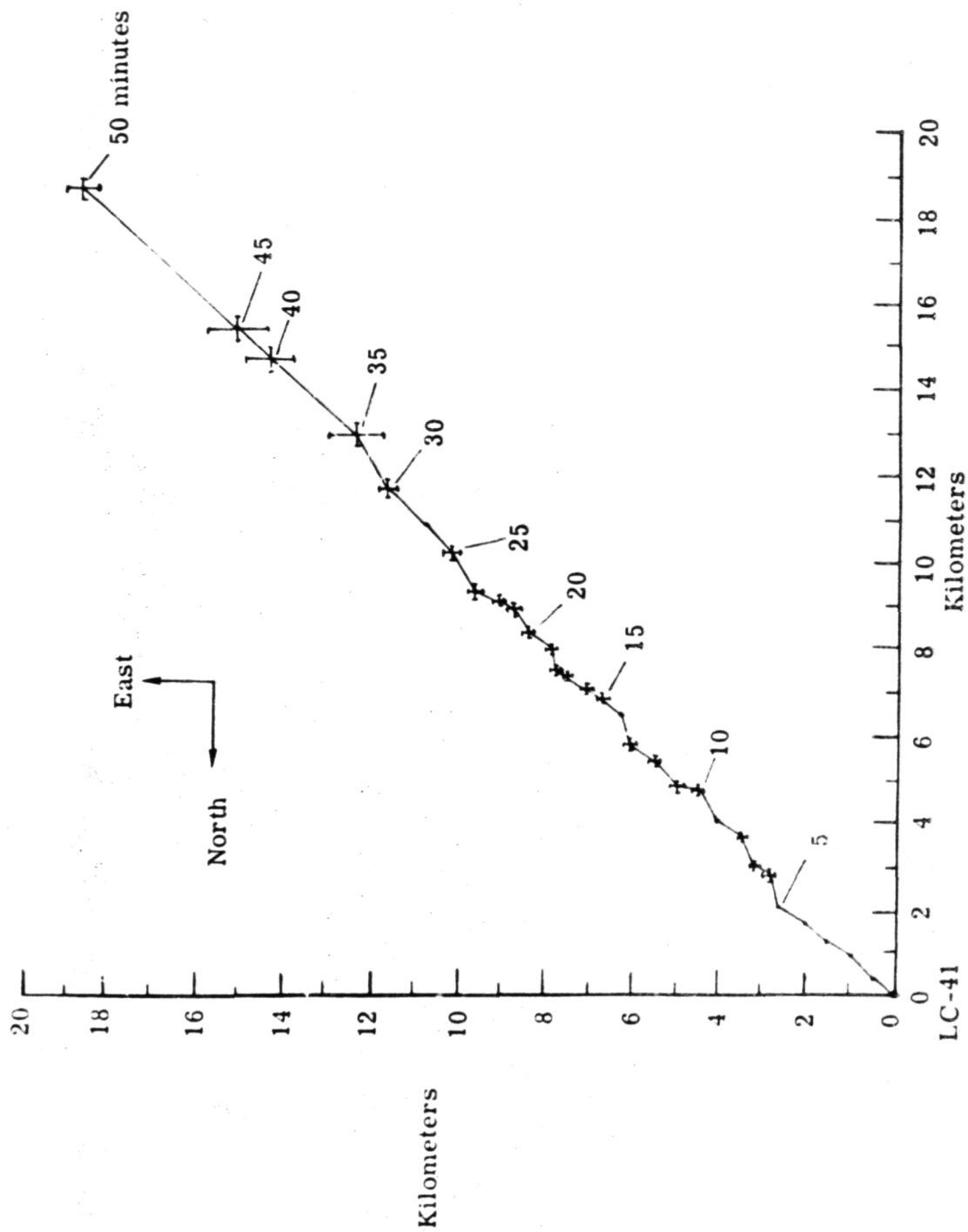
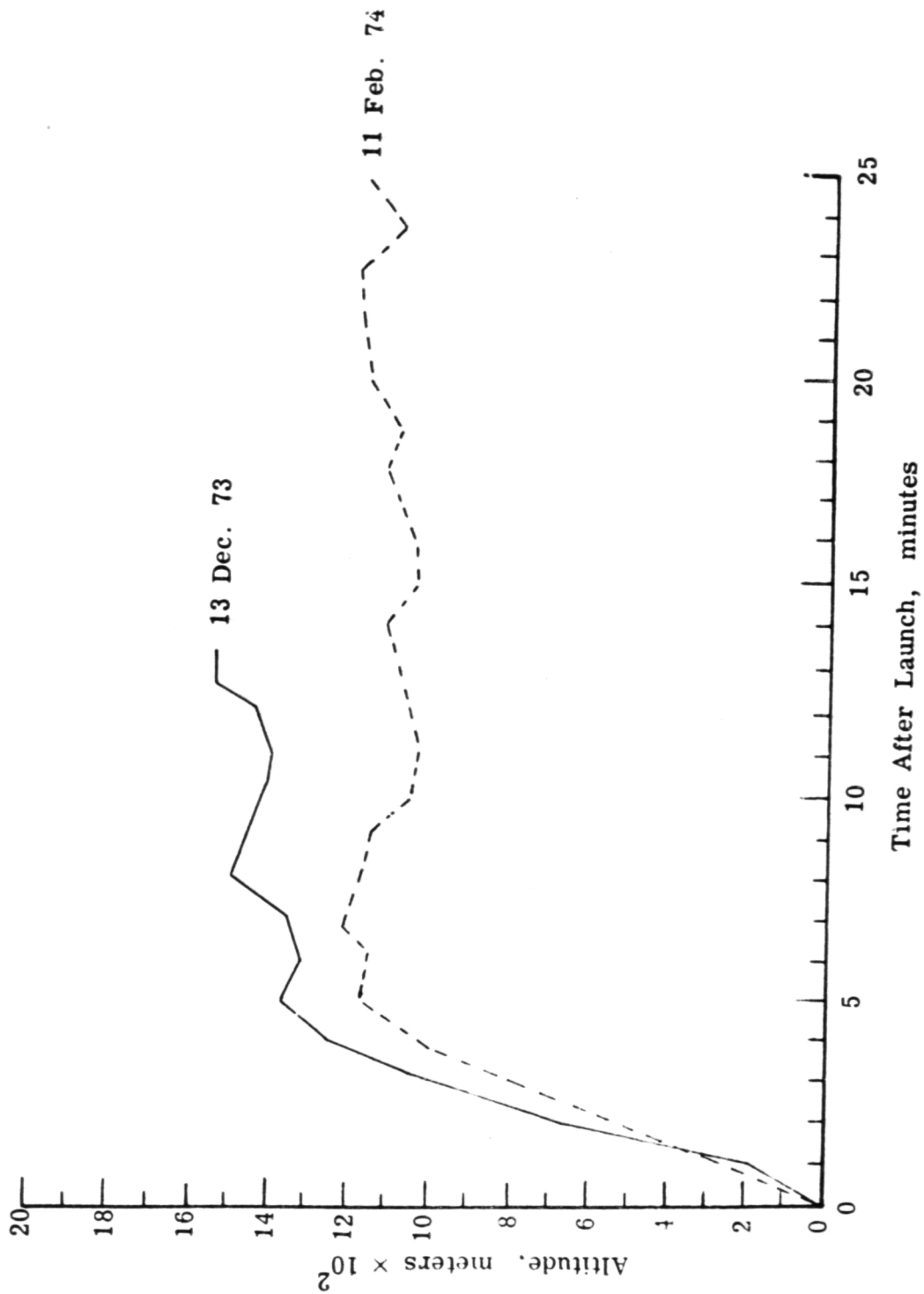


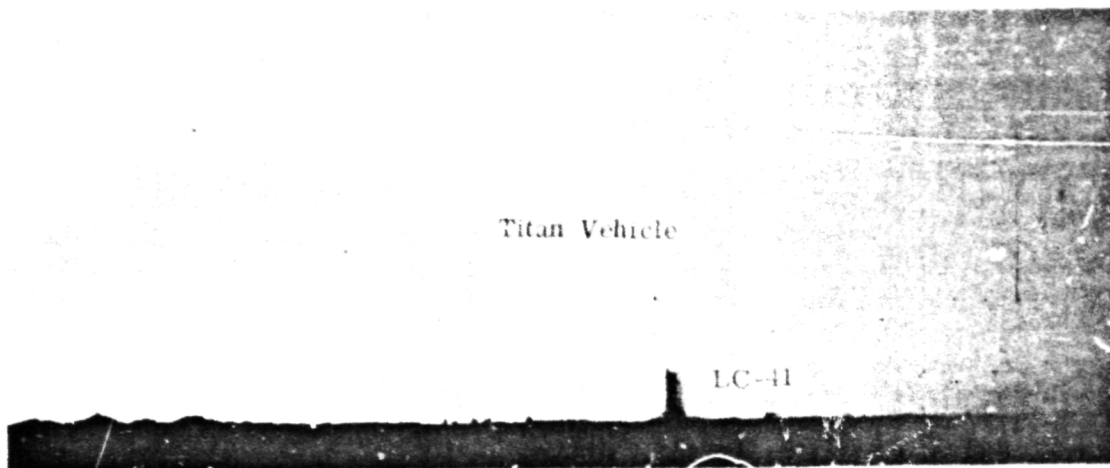
Figure 15. - Titan ground cloud track.



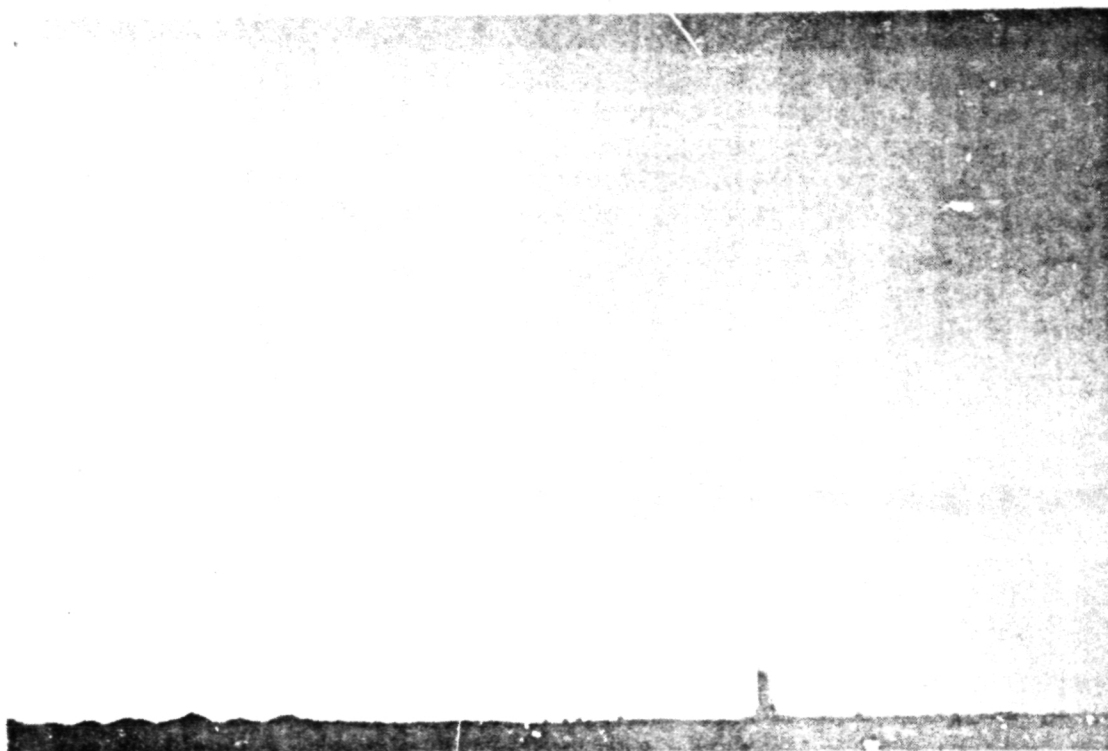
REPRODUCIBILITY OF THE  
ORIGINAL PAGE IS POOR

Figure 14. - Measured Titan III cloud rise to stabilization, KSC launches.

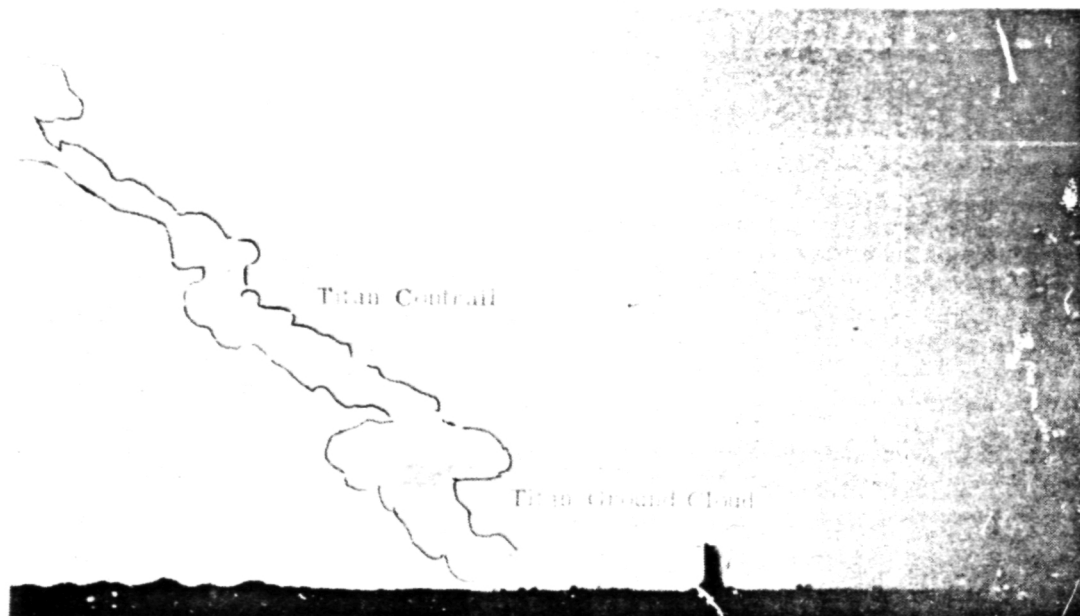




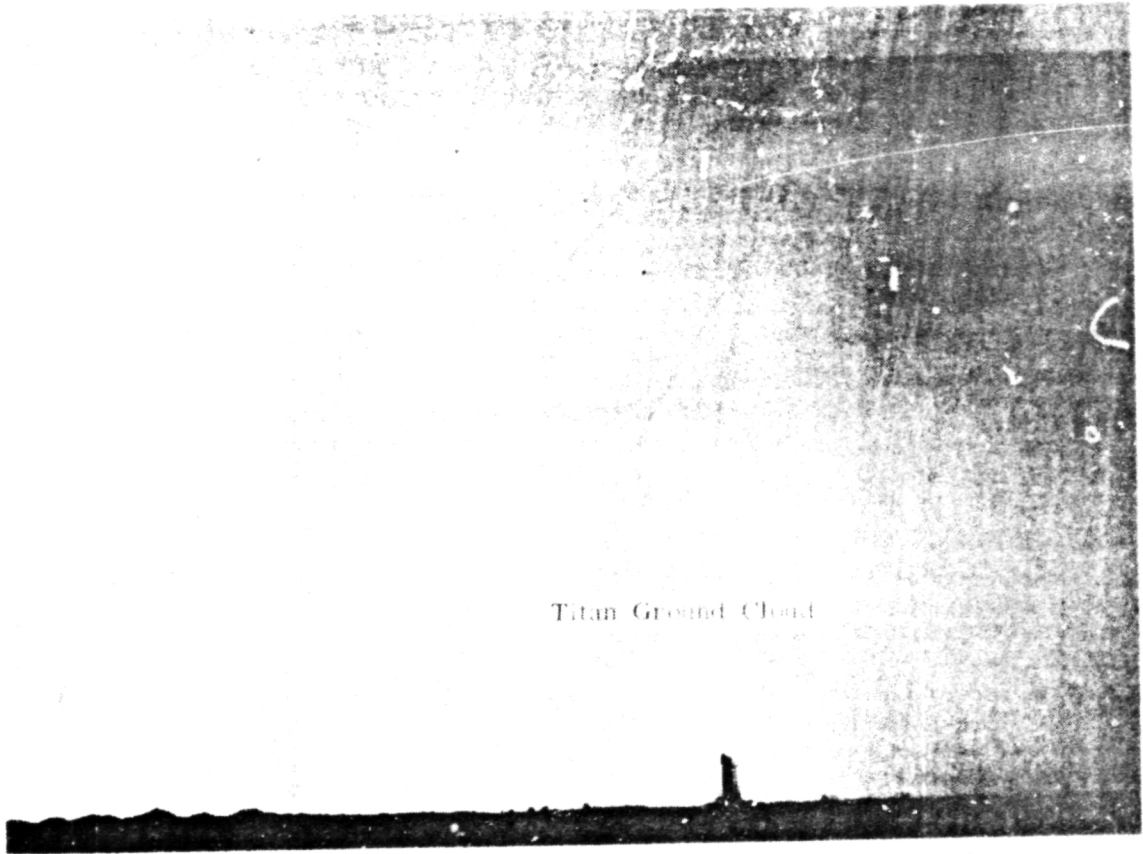
(a) T + 30 seconds



REPRODUCIBILITY OF THE  
ORIGINAL PAGE IS POOR



REPRODUCIBILITY OF THE  
ORIGINAL PAGE IS POOR



Titan Ground Cloud

(c) T + 240 seconds

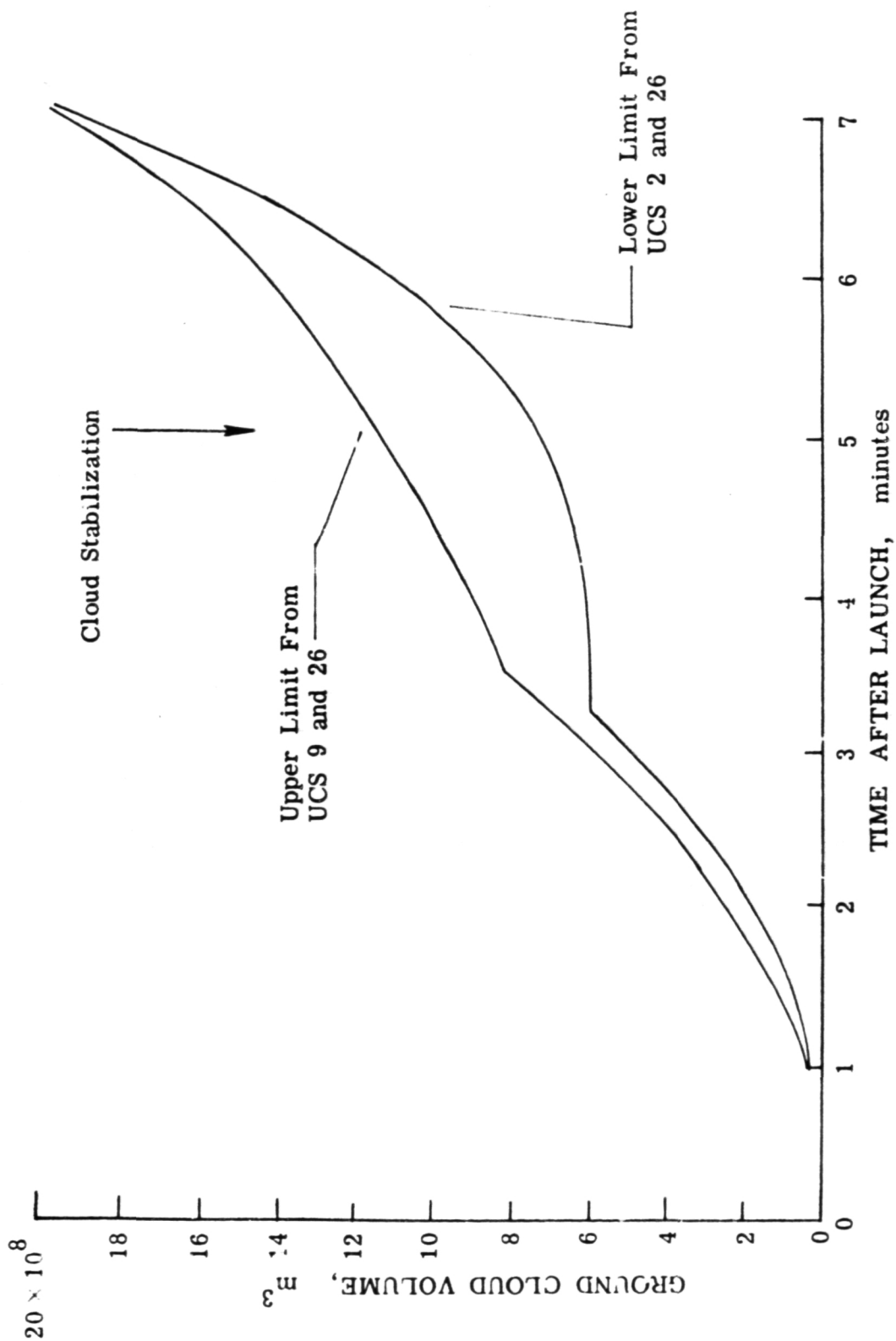
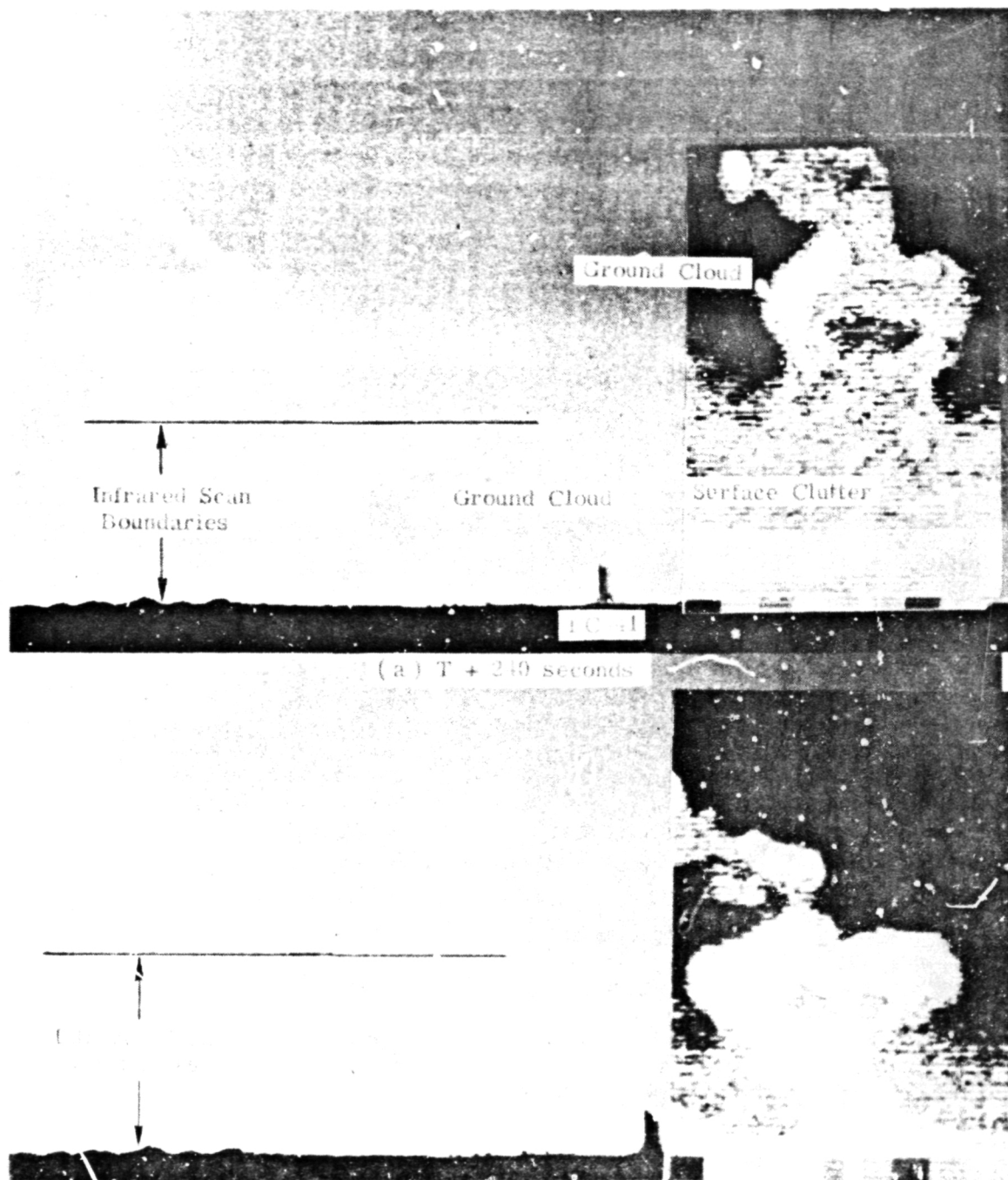
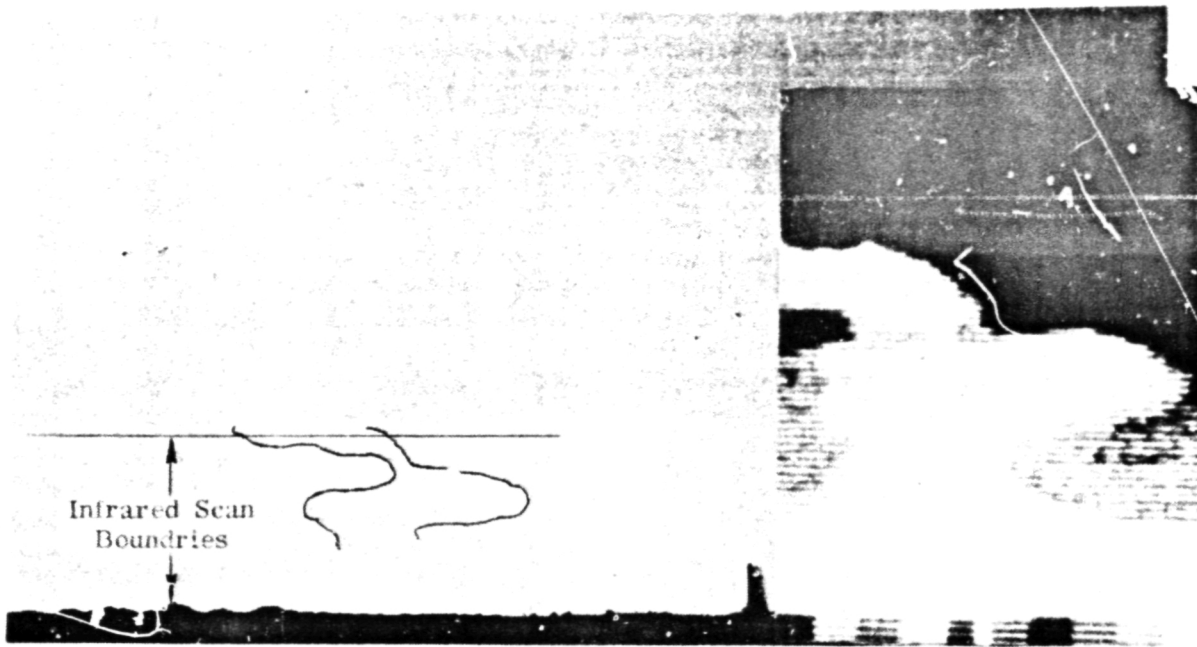


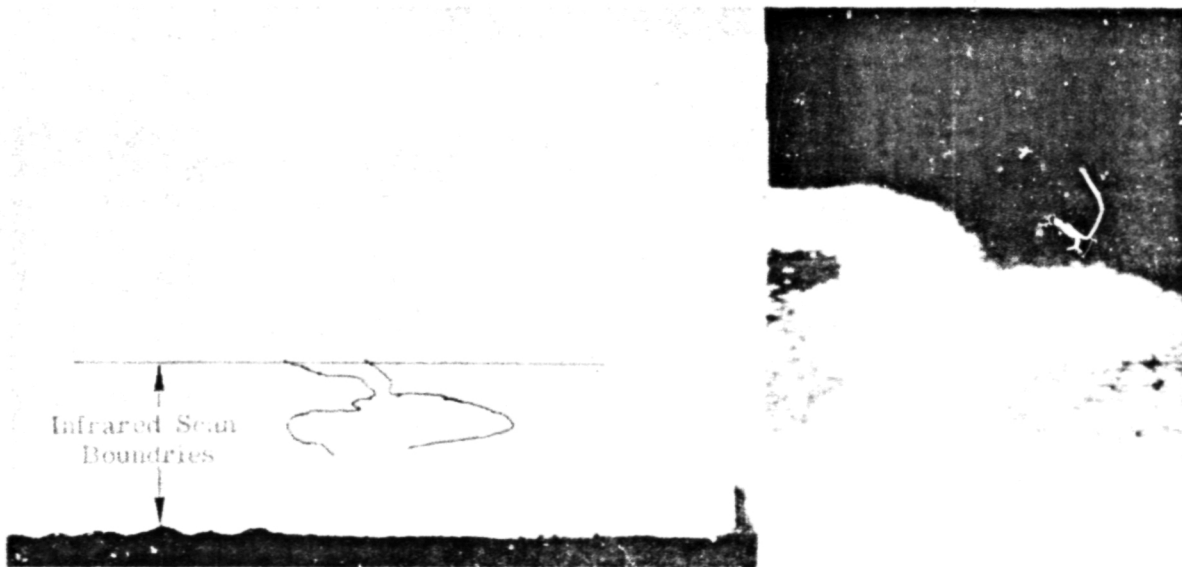
Figure 16. - February 11, 1974 measured Titan-Centaur ground cloud growth.

REPRODUCIBILITY OF THE  
ORIGINAL PAGE IS POOR





(c)  $T + 510$  seconds



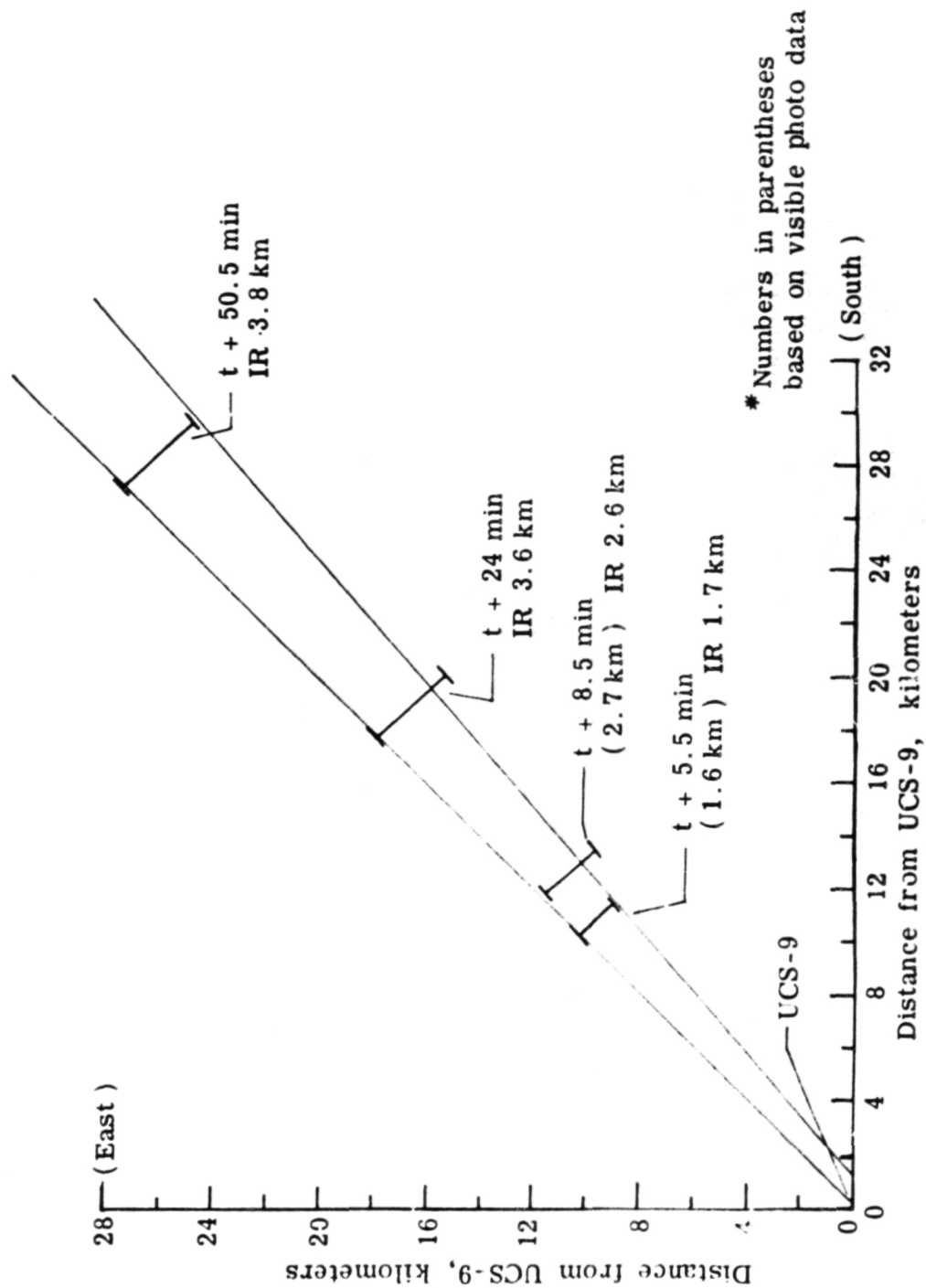


Figure 13. - Measured crosswind cloud growth.

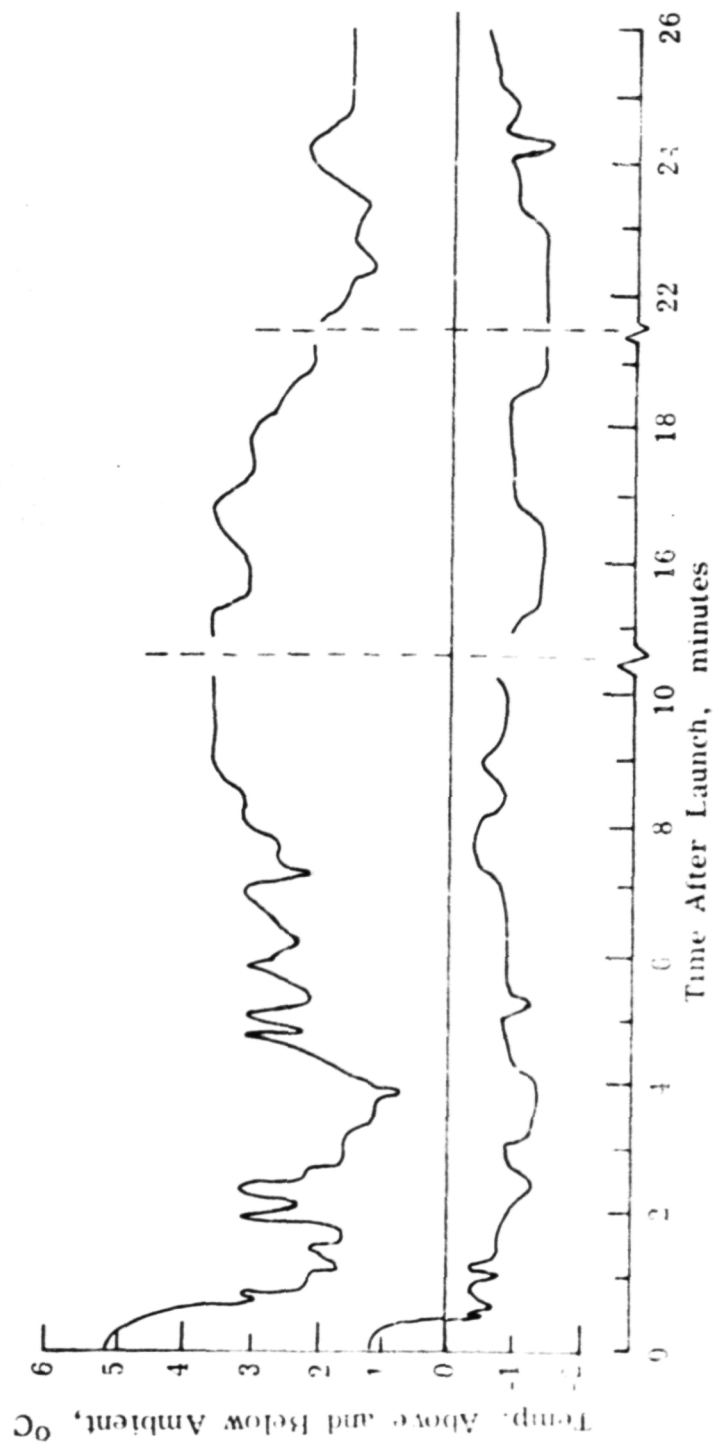


Figure 19. - Cloud temperature range.



**END  
DATE  
FILMED**

**JUN 28 1976**